PERGAMON

Quaternary International 101–102 (2003) 43–65

Geomorphic and geologic evidence of ongoing uplift and deformation in the Mérida Andes, Venezuela

F.A. Audemard M.*

FUNVISIS, Earth Sciences Department, Caracas, Venezuela

Abstract

The Mérida Andes is a mountain chain that trends SW–NE in western Venezuela, extending for some 350 km from the Colombian–Venezuelan border to the city of Barquisimeto. Its highest peaks reach 5000 m in elevation in the central portion, near Mérida. This chain appears to be the northeastward topographic prolongation of the Eastern Cordillera of the Colombian Andes. The latter belongs to the main Andes chain that extends along the Pacific coast of South America. However, there is no direct genetic relationship between the Mérida Andes and Eastern Cordillera. The Mérida Andes uplift is not produced by convergence across a conventional type-B subduction, as most of the South American Andes are. In addition, the Mérida Andes and Eastern Cordillera are separated by the southern termination of the left-lateral strike-slip Santa Marta-Bucaramanga fault, and the NW–SE trending Santander Massif. The present Mérida Andes chain build-up results from Pliocene–Quaternary transpression due to oblique convergence between two continental blocks: South America and Maracaibo Triangular Block. The present geodynamic setting is responsible for ongoing strain partitioning along the Mérida Andes where the foothills and the mountain belt have been shortened transversely in a NW–SE direction whereas the Boconó fault, roughly located in the core and along the Mérida Andes axis, accommodates dextral slip. Tectonic inheritance in the Mérida Andes plays a major role, since the chain growth partly results from inversion of Jurassic (half-) grabens, exposing Precambrian and Paleozoic rocks of the South American continental crust along the chain core.

Evidence of very different kinds attests to the ongoing growth of the chain. From the geomorphic viewpoint, the axial valleys display well-preserved Quaternary staircase terrace systems with more than 500 m of vertical drop between the oldest terrace and present river beds. Rivers cutting across the structural grain of the chain show very distinct transverse ''wine cup'' profiles, attesting to the rapid uplift of the chain. In some cases, rivers have downcut over a 1000 m of relief, where the lower 200–300 m of these profiles exhibit subvertical walls.

Other features that support the significant uplift of the chain and its youth are synorogenic mollasic deposits along both flanks of the chain, deposited in flexural basins, whose thicknesses reach 8 and 3 km on the northwest and southeast of the Mérida Andes, respectively. These continental deposits of essentially Plio–Quaternary age are arranged in up-dip convergence growth wedges, which are being deformed or destroyed by basin-vergent intracutaneous wedges, triangular zones and/or flat-and-ramp structures rooted under the Mérida Andes.

The Mérida Andes core comprises igneous and metamorphic rocks formed at depths of 8–10 km, that are cropping out at its highest summits at about 5000 m elevation, implying a total uplift of the order of 12–15 km in the last 3–5 Ma (average uplift rate of 2–5 mm/a). Activation age and amount of uplift match rather well with those derived from fission-track thermochronology.

The entire mountain belt exhibits widespread seismicity, essentially restricted to upper crustal levels (seismogenic layer). As well, focal mechanism solutions confirm the strain partitioning taking place in the Mérida Andes at present: right-lateral strike-slip along the sub-axial Boconó fault and basinward thrust solutions on both flanks. Underfed/under-destruction pull-apart basins (Las González and Apartaderos) along the Boconó fault appear to be complementary evidence of rapid uplift of the Mérida Andes.

1. Introduction

This paper attempts to place the recent evolution of the Mérida Andes chain (MA) in time and space. Therefore, understanding its role in the present geodynamic setting is needed. In that respect, evidence from very different sources is discussed to demonstrate the youth and the rather rapid uplift rate of this chain, as well as how strain is accommodated.

The Mérida Andes is a prominent geomorphic feature in the landscape of western Venezuela. It extends

*Corresponding author.
E-mail address: faudemard@funvisis.org.ve (F.A. Audemard M.).

1040-6182/02/$ - see front matter © 2002 Elsevier Science Ltd and INQUA. All rights reserved.
PII: S1040-6182(02)00128-3

NW–SE for some 350 km from the Colombian–Venezuelan border to the city of Barquisimeto (Fig. 1). Its maximum width is on the order of 100 km. The MA reaches 5000 m height at the Sierra Nevada, southeast of Mérida in the central Mérida Andes, and is bounded on both flanks by the lowlands of the Maracaibo and Llanos basins on the northwest and southeast, respectively. Two conspicuous foothills are clearly distinguishable along both flanks, although the southeastern one is better developed, extending for over 150 km between Ciudad Bolivia and Acarigua and as wide as 25 km (Fig. 1). The MA seems to be the northeastward topographic prolongation of the Eastern Cordillera (EC) of the Colombian Andes. The latter belongs to the main Andes chain that extends all along the Pacific coast of South America (SA), from Patagonia in Argentina to northern Colombia. However, the MA and EC do not display a direct genetic relationship between them (Fig. 2), as the present Venezuelan (or Mérida) Andes are not related to direct interactions between SA craton and either arc terrains or oceanic domains, as are the remainder of the SA Andes. In addition, both chains are split by the southern termination of the left-lateral strike-slip (LLSS) Santa Marta-Bucaramanga fault (SMBF), and the NW–SE trending Santander Massif (SM). The present chain build-up essentially results from Pliocene–Quaternary transpression due to oblique compression between two discrete continental blocks. This Plio–Quaternary compression is superposed on the first Miocene compressional phase. Together, these have inverted Jurassic (half-) grabens, exposing Precambrian and Paleozoic rocks of the SA continental crust.

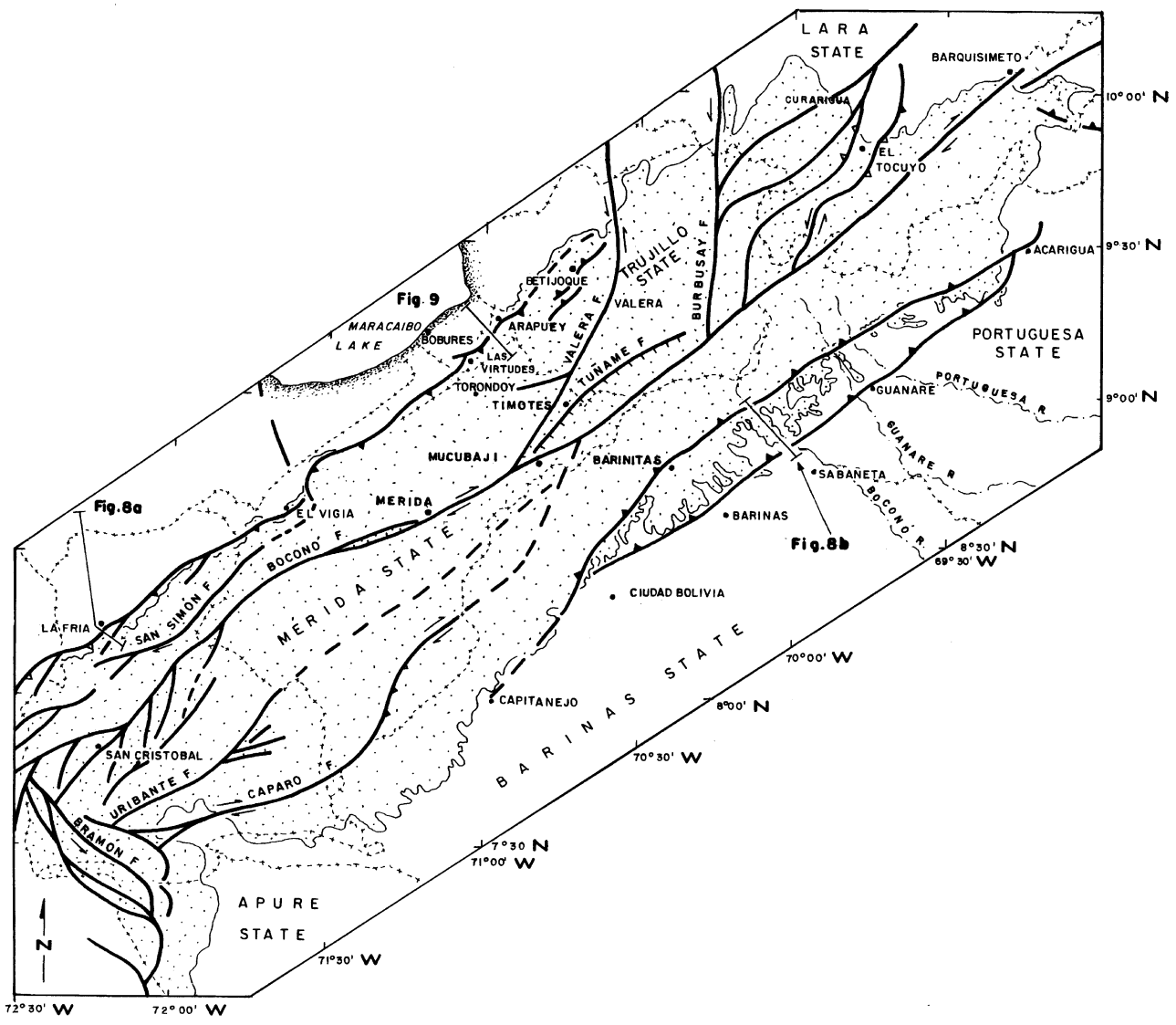

Fig. 1. Major neotectonic features along the Mérida Andes. Notice their variation along strike. Relative location of figures imaging seismic profiles is also shown. For relative location, refer to Fig. 2.

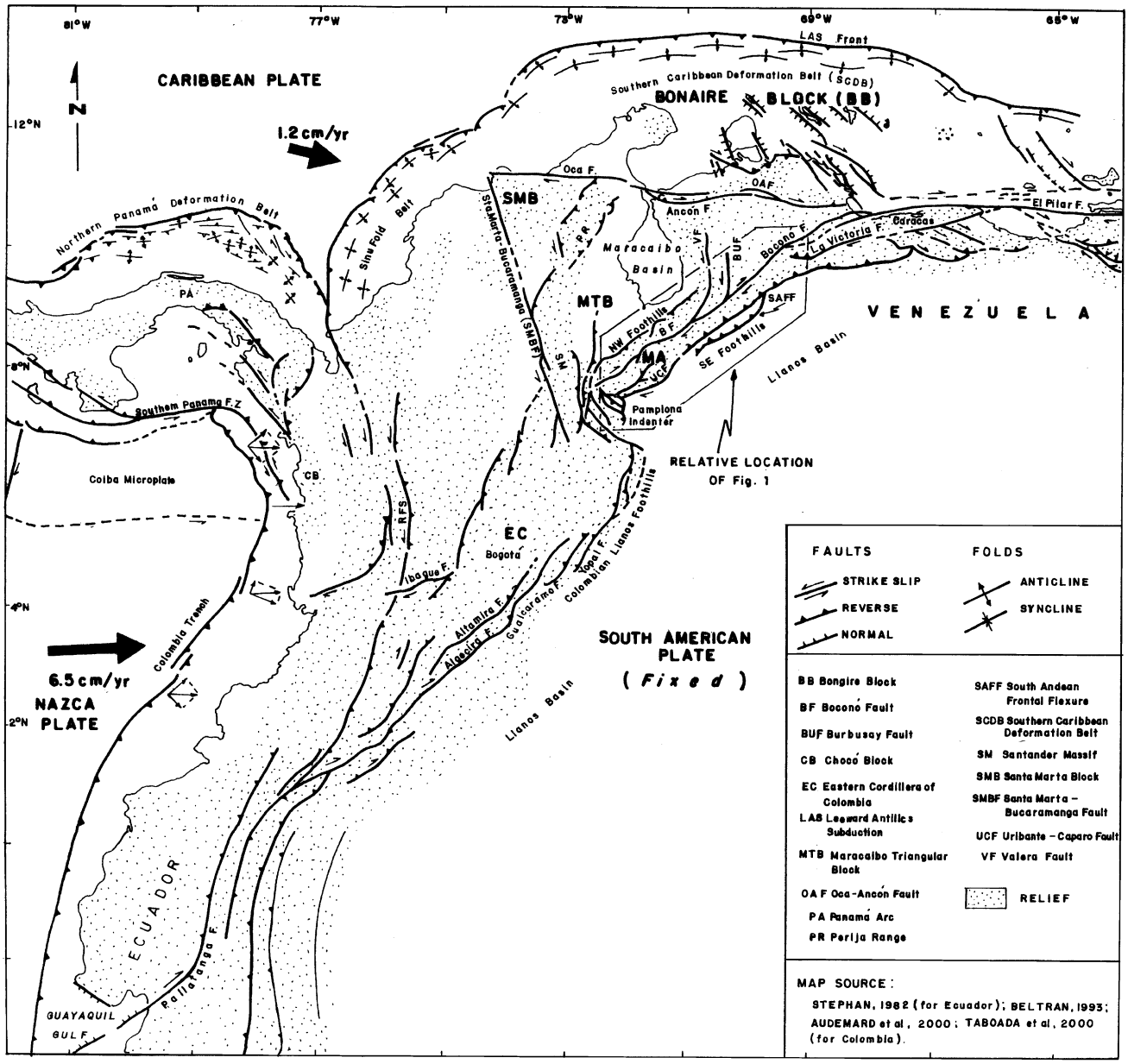

Fig. 2. Mérida Andes (MA) with respect to the geodynamic setting of the northern Andes, from Ecuador to Venezuela. Abbreviations are kept unchanged for all figures and text. Major tectonic blocks are outlined in Fig. 12.

2. Geodynamic setting

As the MA orogeny is not to be attributed to convergence at a conventional type B subduction zone, as occurs in the rest of the SA Andes, this chain needs to be placed within its geodynamic setting in order to understand the chain build-up. Consequently, the Venezuelan Andes (MA) are related to the interaction among the Caribbean, SA and Nazca plates and other minor continental blocks squeezed among the three larger ones. This interplay dramatically varies along strike from east to west (Fig. 2). Whereas northern Venezuela essentially lies in the Caribbean–SA plate interaction zone, western Venezuela shows a more complex geodynamic setting (Audemard, 2000; Audemard et al., 2000). A wide consensus has established that the Caribbean plate moves roughly eastward relatively to SA (Bell, 1972; Malfait and Dinkelman, 1972; Jordan, 1975; Pindell and Dewey, 1982; Sykes et al., 1982; Wadge and Burke, 1983; Freymueller et al., 1993; Kellogg and Vega, 1995; among others), but this active plate boundary is not of the simple dextral type (Soulas, 1986; Beltrán, 1994), since it is an over 100 km wide active transpressional zone (Audemard, 1993, 1998; Singer and Audemard, 1997). Important relief elements (the coast and interior ranges along the

northern coast) are associated with this east–west trending northern boundary. This transpressional boundary (transpression in senso lato) extends southwestward into the MA, where the foothills and the mountain belt have been shortened transversely in a NW–SE direction, whereas the Boconó fault, roughly located in the core and along the MA axis, accommodates dextral slip. Partitioning, both in the Andes and in the northeastern interior range, was described by Rod (1956a) and other researchers, much before the concept was generally put forward. Consequently, the MA fall into a group of chains spread worldwide characterized by stress (or strain) partitioning such as the New Zealand Alps (with the Alpine Fault), Sumatra (with the Great Sumatran Fault), and even the southern SA Andes (with the Atacama fault).

In fact, the plate boundary in western Venezuela is up to 600 km wide and comprises a set of discrete tectonic blocks, independently moving among the surrounding larger plates (Caribbean, South America and Nazca; Fig. 2), among which the Maracaibo triangular block (MTB) stands out (Audemard, 2000). This independent block is bounded by the LLSS SMBF in Colombia and the right-lateral strike-slip (RLSS) Boconó fault in Venezuela, and separated on the north from the Bonaire block (BB) by the RLSS Oca-Ancón fault (Fig. 2). In addition, both the Maracaibo and Bonaire blocks are roughly being extruded to the NNE with respect to SA and are overriding the Caribbean plate north of the Leeward Antilles islands (Fig. 2), where a young south-dipping, amagmatic, flat oceanic subduction has been forming in the last 5 Ma (Audemard, 2000). Extrusion of these blocks is related to the collision of the Panamá Arc (PA) against the Pacific side of northern SA and its later suturing (Audemard, 1993, 1998). Recent results from GPS plate motion studies (Freymueller et al., 1993; Kellogg and Vega, 1995; Kaniuth et al., 1999) confirm the northeastward escape of both blocks relative to all surrounding blocks. This adds amount of convergence along the southern Caribbean deformation belt (SCDB) north of the Netherlands Leeward Antilles to the relative convergence of both Americas.

Other considerations can be put forward regarding the PA collision and later suturing of the Chocó-San Jacinto terrane that acts as an east-directed indenter (after the models of Tapponnier, 1977) to northwestern SA:

(1) maximum shortening across Colombia seems to take place north of a line comprising the WSW–ENE trending RLSS Garrapata and Ibagué faults (located west of Santa Fé de Bogotá; Fig. 2), where the EC is wider and located just east of the accreted terranes;
(2) this indentation drives the northward expulsion of northwestern SA as far south as the Guayaquil Gulf. This case differs from those proposed by Tapponnier (1977) in that the indentation is not perfectly normal to the western free face of SA, thus not allowing symmetrical sideward expulsions. That is to say, all extruded blocks are pushed northward because of initial obliquity;
(3) It also seems that part of the Panamá arc (PA) is extruded to the NNW, driven by the LLSS southern Panamá fault zone and the right-lateral transpressional eastern segment of the northern Panamá deformation belt (NPDB), thus inducing shortening across the latter accretionary wedge (NPDB). In addition, partitioning is also occurring in Colombia, as previously proposed by Gutscher et al. (2000), if attention is paid to the present seismicity of the Nazca subduction and to the intracontinental deformation.

As perfectly identified by Gutscher et al. (2000) and Taboada et al. (2000) from contemporary seismicity depth distribution and tomographic studies, a flat slab subduction lies under Colombia north of 5°N that promotes partitioning where oblique convergence takes place, as is the case along the Nazca subduction (Fig. 2). However, some issues remain unsolved regarding the intracontinental deformation within Colombia and Ecuador, taking into consideration that indentation of the Chocó-San Jacinto terranes into the west side of SA should drive northward extrusions, which would require major RLSS faulting. This is the case for most of the major faults such as the Pallatanga and Dolores (in Ecuador), Algeciras and Guaicaramo (in Colombia) and Boconó (in Venezuela) faults, with the rare exceptions of the Romeral-Cauca fault system (RFS) and the SMBF (both in Colombia). The sinistral slip on the SMBF, as proposed by Audemard and Audemard (2002), results from a differential slip rate of escape between the MTB and the block located southwest of it, known in the literature as the North Andes Block. This latter block, which is bounded by the Romeral-Cauca and the EC Southern Foothills fault systems, is squeezed to a greater extent than those lying to the north (MTB, BB and even the Panamá block) by the Indenter, thus slowing down its northward escape. On the contrary, although considered as a LLSS fault by many authors, slip along the RFS is still matter of intense debate and controversy. It is herein proposed that the RFS exhibits left-lateral and RLSS components north and south of the Ibagué fault, respectively. The slip along this major fault system is conditioned by strain partitioning, where compression normal to the Colombia trench is accommodated by subduction, as suggested by focal mechanism solutions (Gutscher et al., 2000; Jairo Osorio, per.com., 2002), and the parallel-to-trench component varies along strike due to the curved trace of the Nazca subduction along the Pacific coast of Colombia, as illustrated in Fig. 2.

3. Active deformations in the Mérida Andes

The MA exhibits four distinct types of active deformation, but all are linked to strain (stress) partitioning: (1) axial dextral strike-slip along the Boconó fault and related transtensional basins at releasing geometries (overlaps or bends) or deep erosional valleys sitting on heavily fractured bedrock; (2) vertical uplift supported by either erosional or depositional staircased alluvial terraces, disruption of pull-apart basins, or deep transverse-to-chain incision; (3) Plio–Quaternary shortening across the chain, mostly attested to in both foothills and not in the chain core due to lack of young deposits; and (4) seismically induced mass wasting (slides, avalanches/flows) and deep-seated slope instabilities (i.e. gravitational spreading) and earthquake-triggered liquefaction/soft-sediment deformation. Partitioning in the MA (axial wrenching and transverse shortening) is supported by the contemporary instrumental seismicity through focal mechanism solutions, as discussed later in this paper.

4. Boconó fault

The Boconó fault is a spectacular NE–SW trending, dextral fault that extends for about 500 km down the backbone of the MA. It runs slightly oblique to the MA chain axis and bounds the Caribbean Coast range of northern Venezuela on the west, thus extending between the Tachira depression, at the border between Colombia and Venezuela, and Morón, on the Caribbean coast of Venezuela. At its north end at the coast, the Boconó fault exhibits a 45° clockwise bend that allows prolongation into the east–west striking San Sebastián-El Pilar system (Fig. 2). To the south, the Boconó fault connects with the CLFFS (Guaicaramo fault) through the Bramón-Chucarima-Pamplona fault system, after undergoing two opposite right-angle bends (Fig. 2), a structure described as the Pamplona indenter by Boinet (1985) and Boinet et al. (1985). The CLFFS seems to extend as far south as the Jambeli graben (Guayaquil Gulf, Ecuador), thus splitting the northwestern corner of SA from the rest of the continent (Stephan, 1982; Fig. 2).

The Boconó fault has been identified, mapped and characterized rather easily by the large number of along-strike geomorphic features, including a continuous series of aligned 1–5 km wide valleys and linear depressions, passes, saddles, trenches, sag ponds, scarps, and sharp ridges (e.g., Rod, 1956a; Schubert, 1980a, b, 1982; Giraldo, 1985; Soulas, 1985; Soulas et al., 1986; Soulas and Singer, 1987; Casas, 1991; Ferrer, 1991; Singer and Beltrán, 1996; Audemard et al., 1999a). Among these, the alignment of valleys associated with the fault is the most conspicuous feature as it makes the fault easily recognizable and mappable in radar (SLAR) images (Fig. 3).

Since the pioneering work of Rod (1956a), several authors have estimated slip rates along different sectors of the Boconó fault for different time intervals (see Schubert, 1982 for a complete review). In particular, right-lateral offsets of Quaternary features, such as mountainous ridges, drainage channels, alluvial deposits and shutter ridges, range from 60 to 1000 m depending on their age. These offsets yield a Quaternary slip rate between 3 and 14 mm/a. However, studies in the Mucubají area (Schubert, 1980a; Soulas, 1985; Soulas et al., 1986) obtained an average slip rate of about 5–9 mm/a, based on 60–100 m of dextral offset (measurement dispersion depends on authors) of the Los Zerpa moraines, which are radiocarbon-dated at a minimum of about 13 ka (Salgado-Labouriau et al., 1977). More recent studies in this area (Audemard et al., 1999a), where the Boconó fault splays into two sub-parallel strands, have determined 85–100 m of dextral offset across moraines on the southern strand of the fault at three sites (Fig. 4). Conversely, on the northern strand, much smaller glaciers developed on the south-facing slope of the range and only one tongue of ice advanced far enough south to form moraines displaced by the fault. At this locality, there is about 40 m of dextral offset of El Desecho moraine (Fig. 4). Conceivably, these offsets (85–100 and 40 m) have accumulated during the past 15 ± 2 ka. If so, these data yield late Pleistocene–Holocene slip rates for the northern and southern strands of 2.3–3.0 and 5.0–7.7 mm/a, respectively. The Boconó fault shows an overall slip rate between 7.3 and 10.7 mm/a for the past 15 ± 2 ka in the vicinity of Laguna Mucubají. Thus, the southern and northern strands, respectively, carry about 75% and 25% of the 7–10 mm/a net slip rate measured in this sector. These rates are essentially consistent with those predicted by plate motion models of about 1 cm/a, assuming that the Boconó fault is part of the main boundary between the MTB and the SA plate (e.g. Molnar and Sykes, 1969; Minster and Jordan, 1978; Soulas, 1986; Freymueller et al., 1993).

From the Mucubají area, the Boconó fault slip rate decreases towards both ends. South of where the fault is the fastest, average slip rate decreases to 5.2 ± 0.9 mm/a between Mérida and San Cristobal (Audemard, 1997a, b) and as little as 1 mm/a at the Venezuela–Colombia border (Singer and Beltrán, 1996). The apparent lower slip rate may be the result of displacement transfer into the Pamplona Indenter convergence, slip distribution along at least three active strands of the Boconó fault system in the southern Andes, and slip transfer to other sub-parallel active faults, such as the Queniquéa, San Simón, Uribante-Caparo and Seboruco faults, among others (Figs. 1 and 2). The rate reduction is then expressed in a longer recurrence interval between

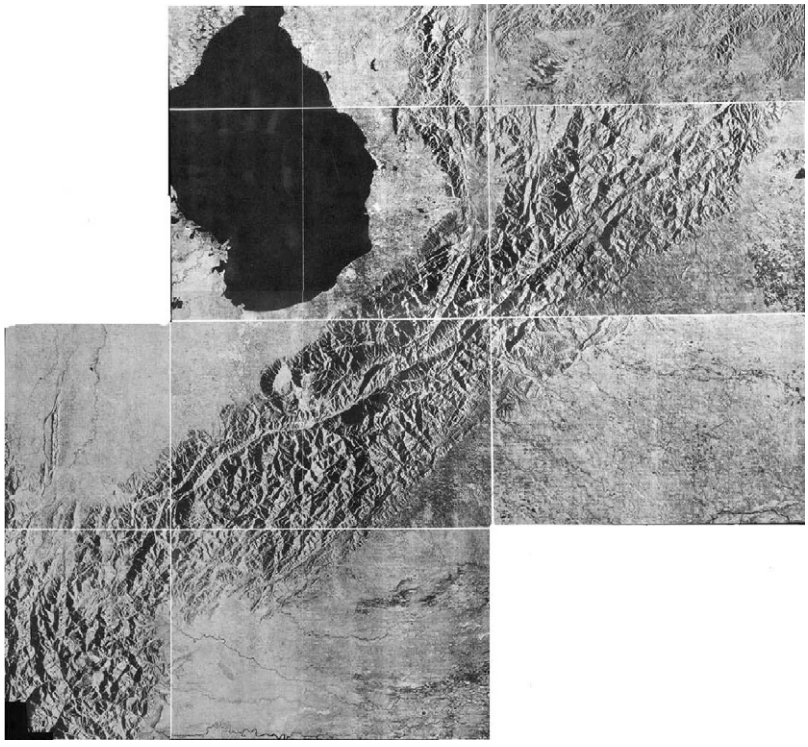

Fig. 3. Radar mosaic of the Mérida Andes, where the alignment of linear valleys outline the location of the Boconó fault, in axial position within the chain, as well as other minor faults such as the north–south trending LLSS faults of Valera and Burbusay, located east of Lake Maracaibo and north of the Boconó fault (after Petróleos de Venezuela, 1992).

equivalent earthquakes on the Boconó fault near Cordero (Audemard, 1997a, b). Similarly, sub-parallel and branching faulting along the northernmost portion of the Boconó fault may explain the slip rate drop (1.5–3 mm/a) reported by Casas (1991), along the Yaracuy valley.

Several pull-apart basins have formed along the Boconó fault, where the appropriate transtensional geometries (bend or relay) occur, and Schubert (1980b, 1982, 1984) has paid particular attention to some of those: Las González-Estanques, Mucuchíes-Las Mesitas and Yaracuy. A discussion on the application of the pull-apart model to some of these basins has been presented by Audemard (1996). Particularly, Casas (1995) and Casas and Diederix (1992) have debated the pull-apart basin origin of the Yaracuy valley, originally proposed by Schubert (1983). However, some other basins have also been postulated, such as Los Mirtos-Zumbador (composite pull-apart west of San Cristobal, Táchira state; Singer and Beltrán, 1996), Cabudare (northeastern edge of the MA, east Lara state; Giraldo and Audemard, 1997) and Apartaderos-Mucubají (central Andes, Mérida state; Soulas, 1985; Audemard et al., 1999a). Two of those particularly deserve our attention because of their connotations as to chain uplift: Las González and Apartaderos.

The Apartaderos basin is 60 km NE of Mérida in the central Venezuelan Andes, and corresponds to a releasing bend of the Boconó fault (Soulas, 1985; Audemard et al., 1999a). Here, the Boconó fault is well preserved along a high-altitude (3500 m) drainage divide that separates the southeasterly flowing streams (Orinoco basin) from the northwesterly flowing streams (Maracaibo basin). This divide is nestled in the area of Laguna Mucubají, belonging to the Parque Nacional Sierra Nevada, one of Venezuela's most spectacular alpine glaciated landscapes. The fault here comprises two conspicuous sub-parallel strands located at about 1–1.5 km apart, both exhibiting magnificent geomorphologic expression (Fig. 4). Schubert (1980b) interpreted the western portion of this area (near Mucuchies, SW of El Cerrito; Fig. 4) as a consequence of a large releasing stepover along the fault, whereas Soulas (1985) mapped the section of the fault between Mucuchies and Los Zerpa as a releasing bend. In fact, this part of the Boconó fault has a slightly more easterly strike with respect to the overall NE–SW trend, supporting Soulas' (1985) interpretation (Audemard et al., 1999a). As well, Funvisis (1999) has postulated that this local transtension at the convergence of the Valera and Boconó faults, as well as the kinematics of the Tuñame fault (dominant normal faulting), is partly induced by the clockwise rotation of the block north of the BF and bounded by the north–south trending LLSS faults of Valera and Burbusay on the west and east respectively, whose kinematics in turn results from a bookshelf rotation

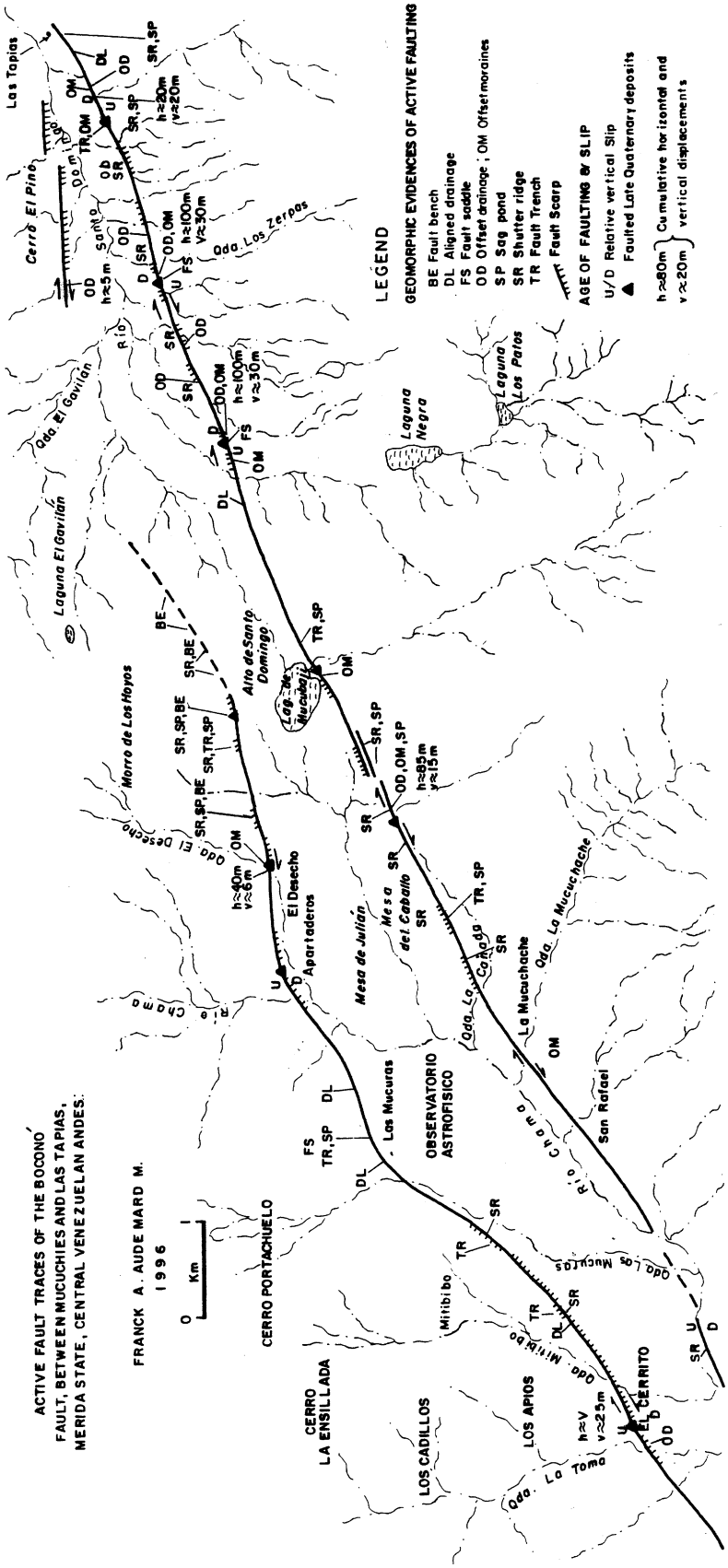

Fig. 4. Active strands of the Boconó fault near the laguna Mucubají, Mérida state, in the MA. The two strands bound the pull-apart basin of Apartaderos-Mucubají that forms at a releasing bend, at the convergence of the Boconó and Valera faults. Notice that Laguna Mucubají points out the location of the water divide between the Chama and Santo Domingo river basins.

mechanism induced by simple shear between the RLSS faults of Oca-Ancón and Boconó. However, although the vertical component of slip appears to be significant at some localities (e.g., from SW to NE in Fig. 4: near El Cerrito, in the village of Apartaderos, Los Zerpas and near Las Tapias), most of the fault geomorphology is typical of a strike-slip fault (Fig. 4). Both fault strands offset latest Pleistocene and Holocene deposits, and fault scarps along the southern strand appear much fresher and more recently formed than in the northern strand (Fig. 5A). The northern fault strand, that bounds the northwest margin of the valley, mainly displays well defined and aligned benches along (or near to) bedrock-cored slopes, but shutter ridges, offset and linear drainages, sag ponds, and fault saddles and trenches are also present at several locations (Figs. 4 and 5B). At present time, this high-altitude basin is being deeply dissected by both the Chama and Santo Domingo river headwaters, whose drainage divide is exactly at the Laguna de Mucubají, even though this depression seems to have accumulated a rather thick sequence of Pleistocene glacial deposits as those preserved at Mesas del Caballo and Julián (Fig. 4). This sedimentary evolution seems to be strongly dependent on marked rainfall changes between glacial and interglacial periods, there is no doubt though that the deactivation of sedimentation in this perched basin is due to generalized chainwide uplift that induces parallel-to-chain axis deep incision along the heavily fractured bedrock or brecciated material generated by the present activity of the axial Boconó fault (Fig. 3).

The Las González-Estanques basin, located just southwest of Mérida, is a mid-to-low altitude (1000–1300 m high) depression within the chain backbone near its highest relief (Sierra Nevada de Mérida located southeast of Mérida city). The basin, produced at a releasing bend of the BF (Schubert, 1980b), is some 50 km long (extending between Mérida and Estanques) and 4.5 km wide at most. It is dominated by ranges about 2000 m higher and contains Quaternary alluvial and lacustrine deposits a few hundred metres thick. This range of elevation contrast is common to most linear valleys sitting on the Boconó and Valera faults. Although being located in a much lower elevation than

Fig. 5. (A) South strand of the Boconó fault at the Apartaderos-Mucubají pull-apart basin, southwest of Laguna Mucubají. White dashed line marks the dextrally offset crest of the El Caballo moraine. Also notice the slide scar in the middle of the picture. (B) General view of the north strand of the Boconó fault at the Apartaderos-Mucubají pull-apart basin, southwest of Laguna Mucubají. This trace displays shutter ridges and dammed alluvial fans or slope deposits behind ridges. (C) Staircased alluvial terraces in the Lagunillas-Estanques pull-apart basin. In the far background, right behind the terraces, the relief is fault-bounded by the northern strand of the Boconó fault. (D) flight of well developed alluvial terraces in the Timotes-Mesa de Esnujaque area. Six levels of alluvial terrace are easily distinguishable in landscape, and at least two additional terrace levels can be proposed from highly eroded remnants preserved as shoulders.

the Apartaderos-Mucubají basin, it is also being cannibalized by deep incision. In this case, dissection is attested by a flight of staircased alluvial terraces (Figs. 5C and 6), partly erosional and partly depositional. Therefore, these basins are being destroyed because generalized chain uplift (or bulk squeezing) prevails over local sagging induced by localized transtension due to the Boconó fault kinematics.

5. Uplift

Vertical uplift in the MA is attested to by several features, among which a flight of either erosional or depositional alluvial terraces, disruption of pull-apart basins, and deep transverse-to-chain incision deserve mention (Fig. 6). As erosion compared to deposition in pull-apart basins has been already discussed above, let us focus next on the two other issues.

5.1. Flights of alluvial terraces

The MA valleys along its major rivers, such as the Motatán, Chama, La Grita, and Torbes, among others, preserve sets of staircased alluvial terraces. Most of these large rivers and valleys, as mentioned earlier, are along major faults (i.e., Boconó and Valera) because the rivers more easily remove brecciated or densely fractured bedrock. Schubert and Vivas (1983) reported that some of these terrace flights have been described by Tricart and Millies-Lacroix (1962); Tricart and Michel (1965); Cabello (1966); Ferrer (1977); Schubert and Valastro (1980) and Lara (1983). These terraces, if depositional, correspond to valley bottom deposits that were later eroded by downcutting rivers, abandoning those alluvial terraces on valley slopes along rivers due to ongoing uplift (Fig. 6). If those are erosional features, they correspond to valley bottoms deprived of any sediment accumulation and they are also abandoned upslope when rivers keep downcutting in search of their equilibrium profiles, that may be repeatedly threatened by tectonic uplift, which is the common situation for a young chain like the MA. The occurrence and type (erosional or depositional) of these features may also change along the longitudinal river profiles. In other words, erosional features can be common in the upstream section where gradient is high (or slope is steep), whereas depositional terraces are formed along the downstream section, but still within the chain. In the upstream section of some of these rivers, the gradient is very high and the valley bottoms are essentially filled by steep alluvial fans and/or debris flows. When the catchment area is above 3000 m in elevation, these valleys contain glacial and/or gelifraction products (Fig. 6). In narrow valleys with steep slopes, the lateral sediment input is commonly as alluvial fans, such as along the Chama River. Some of these terraces can exhibit scarps as high as 100 m or more, as along the airport of the city of Mérida. Another city sitting on a terrace displaying high scarps is Santo Domingo, downcut by the homonym river. Schubert (1976) mentions that the Tuñame terrace is at least 200 m thick under Tuñame village, located in a secondary valley to the Motatán River middle course. Schubert and Vivas (1983) mention that 4 terraces have been identified in most cases, the highest being about 200–300 m above riverbeds. Along the Motatán river in the Timotes region, Schubert (1976) identified at least three terraces with heights of 10–20, 40–50 and above 150 m. However, I believe the number of preserved terraces or terrace remnants is well above that estimate, and the difference in height between the lowest and highest (and oldest) terrace is probably more than 500 m in some cases (i.e., Motatán River in the Timotes region). Here, six alluvial terraces (including the present one) can be rather easily recognized, and 2–3 different higher levels of shoulders (very narrow flat remanents hanging over valleys, occasionally on top of interfluves, corresponding to deeply dissected terraces) can be proposed (Fig. 5D).

The shaping of these flights of terraces is not only controlled by vertical tectonics, because the uplift rate can be considered as a constant compared to the timespan of formation of a terrace, although the uplift can be produced by instantaneous stick slip on active thrusts or reverse faults within or bounding the chain, during each single seismic event. Consequently, they also carry a climatic signature that is rhythmic (alternation of glacial and interglacial cycles or shorter climatic cycles, with the highly probable intercalation of instantaneous catastrophic natural events) and allows the vertical stepping or staircasing of terraces because erosion or sedimentation in the valley floors prevails depending on the amount of runoff. Erosion is high in mountains when the climate is humid (glaciers are small and available water in the system is higher; interglacial stage) and sedimentation is abundant in the foothills. The reverse occurs during the dry periods (glacial stage). So, large episodes of molassic deposition in the foothills are also linked to this climatic variability which is attested to by the occurrence of flights of fluvial terraces downstream as well (Fig. 6).

5.2. Deep river incision

Conversely to the valleys and rivers previously described, some other rivers transversely cut the chain, as well as the major structural trends. Some of these rivers occasionally are very narrow and steep and their valleys are deprived of any sediment along those sectors. These rivers show knickpoints and sectors with very steep gradients. They do not develop a smooth concave

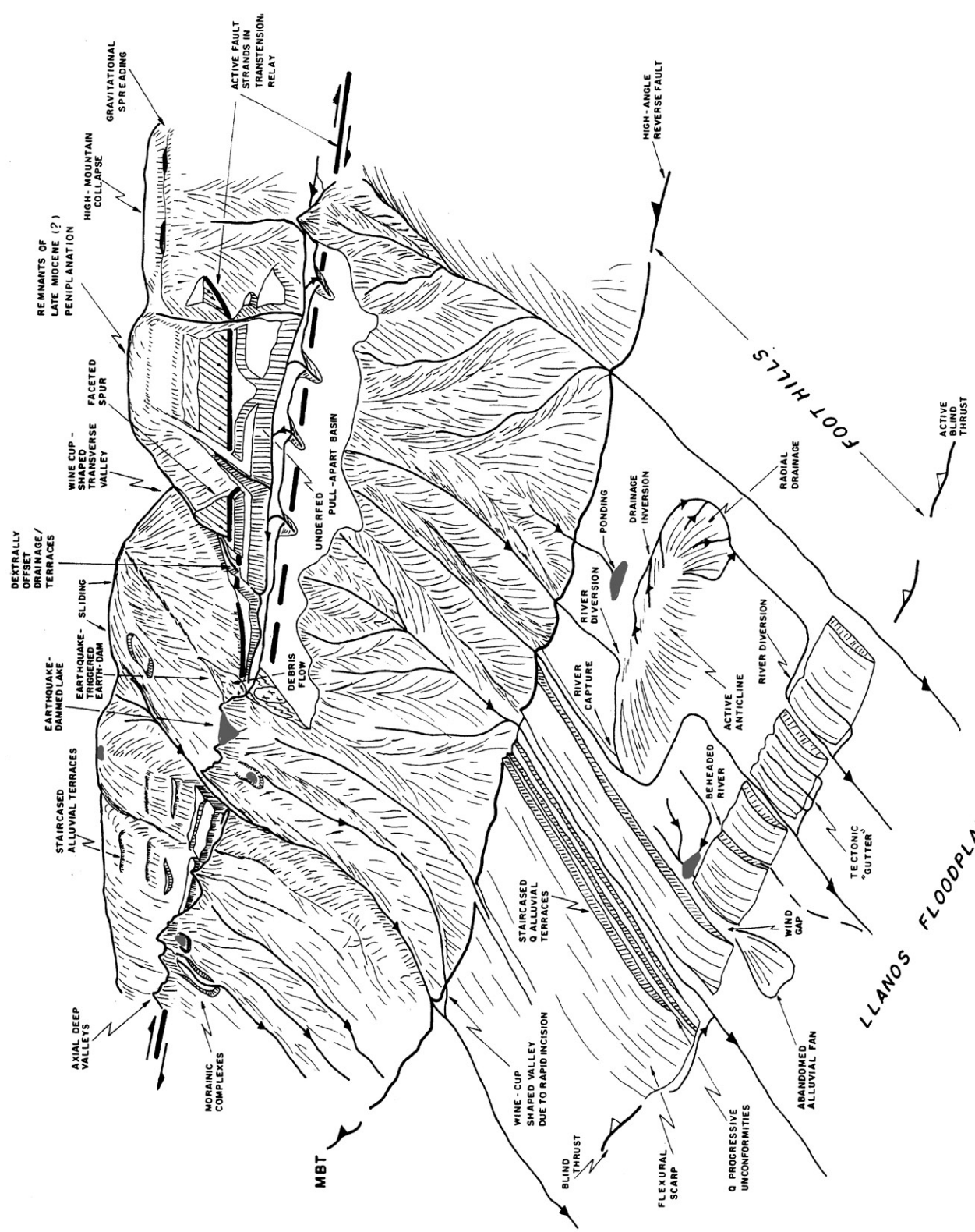

Fig. 6. Idealized block diagram of the Mérida Andes and its southeastern (Llanos) foothills, showing the set of major geomorphic features diagnostic of active tectonics and mass wasting.

Fig. 7. (A) Wine-cup-shaped cross profile of the Santo Domingo, between the dam and Barinitas, in the portion where the river cuts across the NE–SW structural trend of the MA. White lines indicate the steepening of valley slope from top to bottom. Notice as well the presence of waterfalls. (B) Flexural scarp of SAFF (southeastern foothills of the MA), between Guanare and Barinas. The Boconó River gap is visible in the far background as a lighter patch. (C) Beheaded river running across the flexural scarp northeast of Barinas, that is disconnected from the original drainage system blocked behind the eroded upstream side of the flexural scarp, in the foreground. (D) Progressive tilting of the different alluvial terraces along the Boconó River at Puente Páez, between Guanare and Barinas. The older and the higher the terrace is, the steeper the surface of the terrace looks.

longitudinal profile because the rivers are unable to reach equilibrium. Incision is usually very prominent, producing very narrow valleys bounded by subvertical walls at the bottom, as high as 200–300 m in elevation. River downcutting easily surpasses 1000 m in elevation across rather "fresh" rock. Tributary drainages very frequently exhibit waterfalls (Fig. 7A). The valley cross profile of these rivers exhibit "wine-cup" shapes, which is unequivocal evidence of very rapid uplift (Figs. 6 and 7A).

6. Foothills

The MA foothills are areas where transverse shortening is conspicuously attested. As mentioned earlier, strain partitioning is taking place throughout the MA. Thus, significant thrusting occurs sub-parallel to the RLSS Boconó fault on both sides of the MA, accommodating a rather large amount of shortening across the chain (González de Juana, 1952; Rod, 1956a; Hospers and Van Wijnen, 1959; Schubert, 1968; Kellogg and Bonini, 1982; Henneberg, 1983; Soulas, 1985; Audemard, 1991, 1997a, b; De Toni and Kellogg, 1993; Jácome, 1994; Sánchez et al., 1994; Colletta et al., 1996, 1997; Duerto et al., 1998).

A good knowledge of the sub-surface structure of both foothills has been acquired due to the large set of geophysical surveys performed in the Maracaibo and Barinas-Apure basins by the oil industry in the last two decades, but most of the deep structure of the chain remains unknown except for the Moho depth in certain areas (29 km for the Maracaibo crust by Padrón and Izarra, 1996) and the general mass distribution that may be derived from gravimetric profiles and surveys (e.g., Hospers and Van Wijnen, 1959; Bonini et al., 1977).

The seismic surveys confirmed the dominant NW vergence of the MA, because a rather deep conventional flexural basin developed on the northwest (the Maracaibo basin; Fig. 8A). A much shallower flexural basin

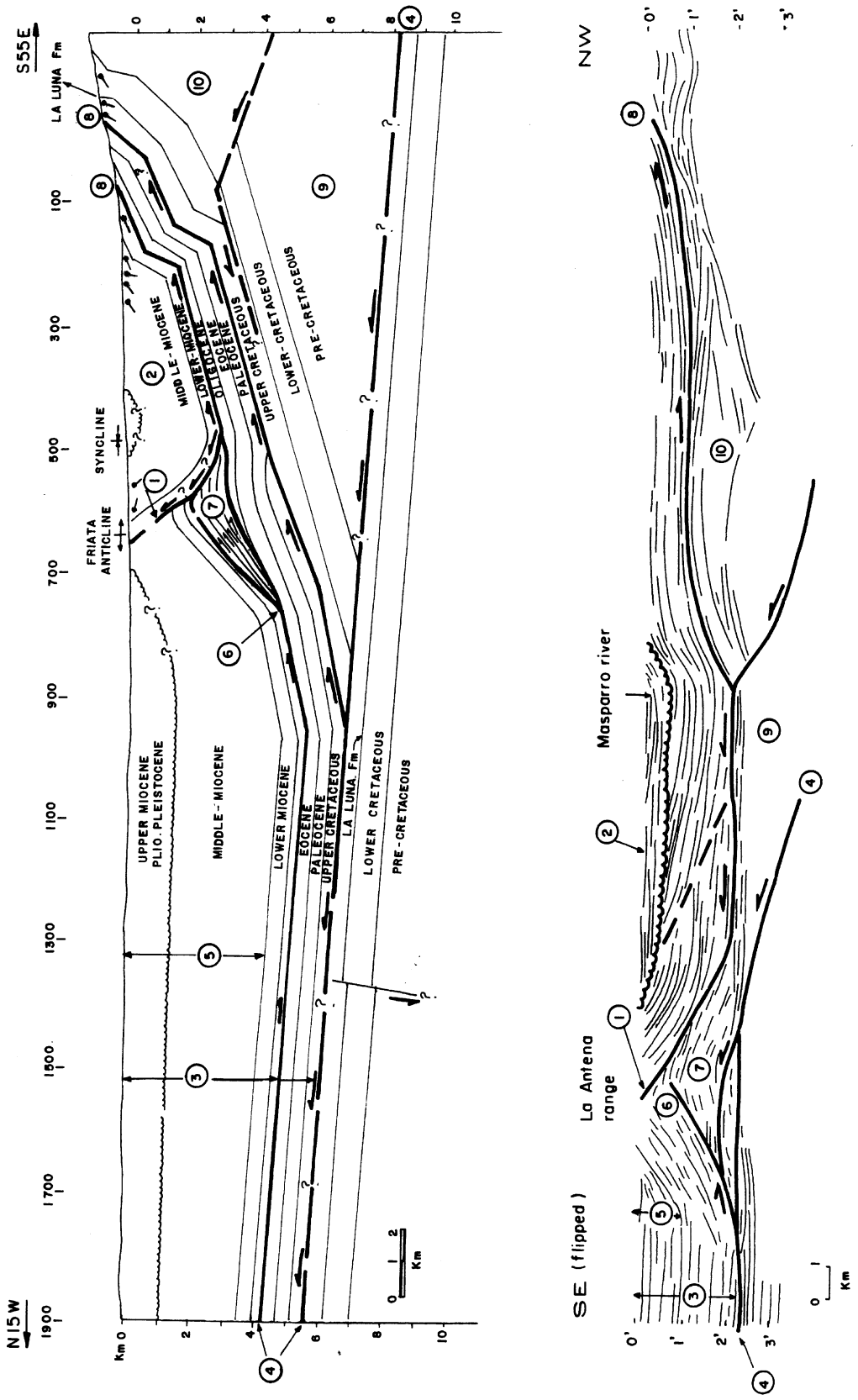

Fig. 8. Many similarities regarding structural styles may be observed between both Mérida Andes (MA) foothills (comparison indicated by labelling): (A) structural interpretation across the western foothills at La Fría (after De Toni and Kellogg, 1993; refer to Fig. 1 for location) and (B) line drawing across Las Garzas—Fila La Antena or Peña Larga—anticline in the eastern foothills (after Funvisis, 1997and Audemard, 1999).

formed to the southeast, although SE-thrusting has been identified within the Tertiary sedimentary sequence, mainly northeast of Barinas (Fig. 8B).

6.1. Northwestern foothills

Although the northwestern Andean thrust front of the MA exhibits a well-developed NW vergence, these foothills may be subdivided into two distinct provinces (Audemard, 1991). A southwestern segment southwest of El Vigia is associated with a major passive roof backthrust decoupled from the Upper Cretaceous Colón Formation, where the overlying Tertiary sedimentary sequence dips NW at high angle in a belt some 10 km in width along the foothills. The upper part of this sequence, comprising the Late Miocene Isnotú Formation and the Plio–Pleistocene Betijoque Formation, displays a chainward-pinching out (upward convergent) wedge where onlaps of seismic reflectors evidence several progressive unconformities. In fact, this molassic wedge dates the growth and uplift of this flank of the MA and the syntectonic sedimentary package is essentially Late Miocene to Pleistocene in age. Under this wedge and above the deepest decollement in the Colón shales, two other decollement levels are interpreted by Audemard (1991) and (De Toni and Kellogg, 1993; Fig. 8A) within the thin Eocene–Oligocene sequences and between the Lower and Middle Miocene markers, respectively. The SE-backthrusted sequence soles in the Colón Formation, and is decoupled by a NW-vergent four-basement-thrust-sheet stack that acts like an intracutaneous wedge.

The northeastern segment is defined by a major NW verging thrust sheet (Las Virtudes; after Fig. 57 of Audemard, 1991), which acts as a shallow intracutaneous wedge and partly overrides the Tertiary section (Fig. 9). The Upper Miocene–Pleistocene molasse fed by the continuous erosion of the rising MA reaches its maximum thickness of about 8 km near Torondoy (refer to Fig. 1 for location). At the Avispa massif, the Las Virtudes overthrust brings Precambrian and Paleozoic metamorphic rocks (Andean basement) in contact with Tertiary rocks at the mountain front. The thrust is capped by a synorogenic sedimentary wedge containing unconsolidated Plio–Pleistocene sediments of the Betijoque formation that exhibit the same up-dip convergence wedge as in the southwestern segment (Audemard, 1991; Castrillo, 1997). This wedge constrains the emplacement age of the shallow sheet as Late Pliocene, but an underlying deactivated triangular zone also dates, as for the southern portion, the orogenic onset at the Late Miocene (Audemard, 1991).

Along the northwestern foothills, the northeastern portion of the front shows a more advanced stage than to the southwest, implying more shortening, where the large basement-thrust-stacked intracutaneous wedge (still active in the southern portion) is being destroyed by a shallower basement-involved thrust (Audemard, 1991). This also indicates the existence of out-of-sequence thrusting in the northeastern segment of these foothills.

6.2. Southeastern foothills

There is no general agreement regarding the thrust vergence along the southeastern foothills, probably due to masking introduced by triangular zones and intracutaneous wedges, combined with important along-strike variations. For instance Audemard (1991, 1997a, b) proposes that the segment southwest of Barinas displays a predominant NW vergence (e.g., Fig. 2 in Audemard, 1997a, b) but some authors (i.e., Colletta et al., 1996, 1997) believe that such vergence only occurs at shallow crustal levels, thus being a conjugate imbricated thrust system (backthrust) to a deeper SE vergent thrust. For other authors (Rod, 1960; Stephan, 1982; Castrillo,

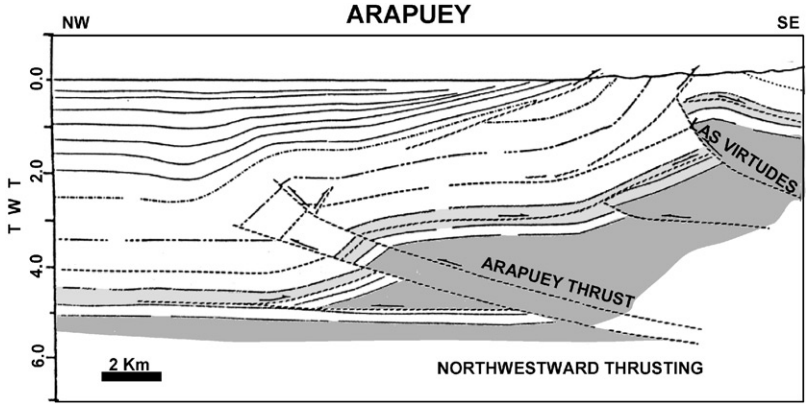

Fig. 9. Schematic NW–SE profile across the Avispa massif and Las Virtudes thrust, in the western Mérida Andes foothills, showing a shallow intracutaneous wedge and the still active synorogenic up-dip convergent growth wedge essentially comprising the Late Pliocene–Quaternary Betijoque Formation. Also notice the underlying fossil triangular zone (after Audemard, 1991, 1997a, b).

1997; Duerto et al., 1998), this foothills vergence is SE directed. Several authors (Giegengack, 1984; Jácome, 1994; Sánchez et al., 1994) even propose dual vergence.

The eastern foothills may show different behavior along strike, the dividing line being somewhere between Capitanejo and Barinas (refer to Fig. 1 for location). The southwestern portion of the southeastern foothills shows a dominant NW vergence with secondary conjugate backthrusting, which is all related to the Pamplona Indenter. The Pamplona Indenter is responsible for convexly bending the southwestern portion of the MA and simultaneously pushing the Boconó fault trace off its axial position. Conversely, the northeastern portion of these foothills exhibits a SE vergence, at least in the upper crustal levels, as demonstrated by Funvisis (1997), Duerto et al. (1998) and Audemard (1999). This thrusting even deforms the Plio–Quaternary molasses (Audemard, 1991, 1999; Funvisis, 1997), as indicated by a very prominent NE–SW-trending, SE-facing flexural scarp—South Andean frontal flexure (SAFF)—that defines the boundary between the foothills unit and the Llanos plains (Figs. 1, 6 and 7B). This flexural scarp and other minor geomorphic features of ongoing compressional tectonic activity shall be discussed later in this paper. These flexural scarps grow at the front of active fold-and-thrust belts where deformation is dominated by thin-skinned tectonics, though all ramps are ultimately rooted under the Andes (overall thick-skinned tectonics). The thrusts at upper levels are gently dipping and form both flats and ramps (Fig. 8B).

As structural styles of deformation along both mountain belt edges are similar to a certain extent (Fig. 8), the radical difference in overall shape between both flexural basins needs to be related to the chain load itself. The Maracaibo basin is a rather narrow and short but deep depocenter. In contrast, the Llanos flexural basin is a long, very wide but much shallower basin. This flexural basins geometry directly responds to chain load on top of the overridden basement. When the mountain belt is loading over a large area of the basement, the resulting flexural basin is wide and shallow. On the contrary, when loading is localized on the edge of the overridden basement under the same load, the basin is narrow and deep. A springboard is a good analogue to an elastic lithospheric plate being loaded. If a swimmer stands at the tip of the board, the board only flexes near the free tip, although bend radius is short. On the contrary, if the same swimmer lies flat on the springboard (load is kept unchanged but better distributed), most of the board flexes but it exhibits a smooth bending. Consequently, the shape of the related flexural basins suggests that the deeper structure of the MA chain is definitely asymmetric, where the major northwestern bounding reverse faults need to dip steeper that its SE counterparts, as proposed by Audemard (1991) and Colletta et al. (1997). Another implication is that the MA has been more overthrusted to the SE than to the NW.

Along these southeastern foothill areas, the most frequent and best exposed geomorphic evidences of ongoing compressional tectonics in the associated fold-and-thrust belt are (Audemard, 1999): (1) flexural scarps; (2) drainage patterns and anomalies, and (3) progressive deformation with increasing time. Collectively, these features provide firm evidence for active deformation of the Llanos (southeastern) foothills of the MA. The drainage patterns and anomalies, which reflect very subtle topography modifications, include staircased alluvial terraces exclusively present in the hangingwall block (Fig. 6).

6.2.1. *Flexural scarps*

Flexural scarps are the most conspicuous evidence of gently dipping thrust systems observed at the front of the fold-and-thrust belt along the Llanos foothills. The flexural scarps define the boundary between the foothills unit and the Llanos plains (Figs. 1 and 6). The SAFF in the MA southeastern foothills, a roughly NE–SW-trending SE-facing flexural scarp, extends for over 200 km in length, between the cities of Ciudad Bolivia and Acarigua, and its maximum height reaches 300 m above the rather flat topography of the Llanos plains (Figs. 1, 6 and 7B). Lateral continuity of this scarp is interrupted by large drainage channels, such as the Boconó and Guanare rivers. Those river gaps coincide with the lateral terminations of active individual ramps, as suggested by the extent of the exposed Paleogene rocks within the foothills unit (refer to the geologic map of Venezuela by Bellizzia et al., 1976). This has been confirmed by a 3-D seismic survey across the Venezuelan Llanos foothills, as interpreted by Duerto et al. (1998). Several localities along the Venezuelan SAFF image flexing of coarse early to middle-Pleistocene alluvial deposits, such as in the cities of Guanare and Araure-Acarigua (Fig. 10), as well as along the banks of the Caro and Ospino rivers near the main Llanos road (Funvisis, 1997). The flexural scarps form in association with rather shallow triangular zones that are in turn related to NW-gently dipping thrusts that exhibits flats and ramps (Fig. 8B). It would seem that the Llanos foothills was all uplifted as a single unit, as suggested by the formation of a staircased alluvial terrace system in the hangingwall block, although piggy-back basins are also forming (Fig. 8B).

6.2.2. *Drainage patterns and anomalies*

Drainage or drainage pattern analysis may allow detection of vertical motion in a given area, as mentioned earlier. A comparative analysis is required because all rivers do not respond the same way depending on their size, although they may show similar longitudinal profiles. Generally, big rivers often cut

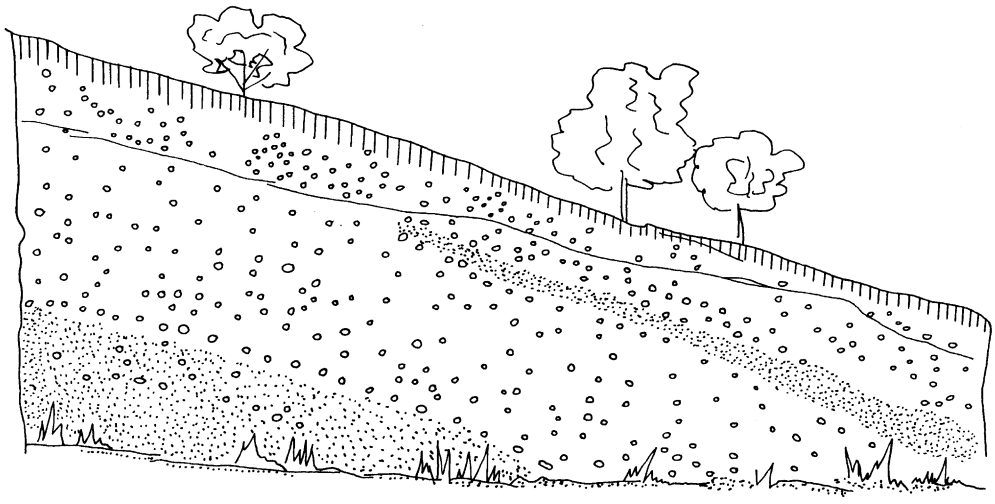

Fig. 10. Outcrop across the South Andean frontal flexure (SAFF) at Guanare, that exposes two different Quaternary alluvial deposits in clear unconformity relationship.

across uplifting structures rather easily without modification of their course. Conversely, small rivers reflect much more subtle topographic modifications than larger rivers in straightforward response to their respective stream power or erosional rates. Nevertheless, big rivers also bring relevant information regarding the uplift history of a region. The most common of these tectonically induced anomalous drainage behaviors (refer to Audemard (1999) for further details; Fig. 6) are: radial drainage, densely dissected morphological scarps, river pattern inversion with flow from basin to range, river diversions, beheaded drainage (Fig. 7C) and stream captures, changes in incision depth and river gradient along river course, dammed creeks and rivers, wind gaps (abandoned river gaps), imbalances between current river flow and river gaps and rivers that are parallel and close to the thrust front on the downthrown block (i.e., tectonic "gutters") and abandoned alluvial fans downstream of uplifting structures. These changes are superposed on an increase of tilt of ground surface or stratigraphic dip with increasing age of Quaternary alluvial ramps and even older formations (progressive unconformities; Fig. 7D).

7. Mass wasting and slope instabilities

Not much stress on this issue is herein desired because these processes are not directly linked to tectonic stresses, although they may be induced by earthquakes and are strongly dependent on gradient (which is a function of relief), slope angle, underlying geologic structures, and so forth. However, it is important to indicate that mass wasting within orogens affects landscape evolution much more significantly than linear or runoff erosion, because mass transfer downslope is more effective although rivers have the subsequent task of redistributing or mobilizing loose materials further downstream. Debris flows, deep-seated slides and gravitational spreading are common processes within the MA (Fig. 6). The two first processes can be either triggered by heavy rainfall (long-lasting antecedent rain followed by short but heavy flush rain is the best triggering hydrometeorological mechanism) or by moderate-to-large local earthquakes. Combination of both triggering agents (prolonged rainy season and seismic activity) is the most effective mechanism, as in the Burgua range, Táchira State, during the Nula May 1994 earthquake. In some cases, debris flows in the MA have dammed rivers during earthquakes, as was the Mocotíes River during the La Grita 1610 earthquake (Singer and Lugo, 1982; Ferrer and Laffaille, 1998; Singer, 1998). Conversely, gravitational spreading (collapse of high mountain areas by lateral flattening) can be simply induced by deep parallel-to-chain river downcutting, since two large sub-parallel free faces along a high relief are needed. This process can be initiated, eased or accelerated by earthquakes, but the seismic activity is not strictly necessary.

Besides the direct permanent ground deformation (surface fault rupturing) and its cumulative expression in landscape by repeat of earthquakes (geomorphic evidence of active faulting), moderate-to-large earthquakes induce other phenomena gathered under the name of indirect permanent ground deformations that include soil liquefaction (soft-sediment deformation) and mass wasting of very diverse types (deep-seated and shallow slides, falls, flows, lateral and gravitational spreading). Some of these permanent features are also been utilized to determine the seismic history of a fault or region, beyond the simple trenching of active surface faulting. At present time, attention in this regard is paid to both

deep-seated slides and soft-sediment deformation (including soil liquefaction and lateral spreading) along the Mucubají sector of the Boconó fault (Audemard et al., 2001). It is worth mentioning that other indirect ground deformations than earthquake-induced effects (sliding and soil-liquefaction) are recorded in the landscape and belongs to the set of geomorphic evidence used to identify structures that do not necessarily crop out (blind thrusts and subduction slabs) or induce large-scale phenomena such as uplifting and bulging. Among those are all the features described above in the Llanos foothills that attest to ongoing shortening across the chain and relate the MA uplift to tectonic forces, as well as the evidence brought by preserved flights of alluvial terraces, deep and quick river incision (wine-cup-shaped cross-section of river valleys) and even the disruption of active pull-apart basins sitting within the chain under uplift.

8. Seismic activity

The Boconó fault zone has been cited as responsible for most of the largest MA earthquakes, as Rod (1956b) initially stated. Cluff and Hansen (1969) have also indicated the same conviction for both historical and instrumental earthquakes (refer to pages 5–13 through 5–16, and 5–45). Among the large historical earthquakes in the MA, Cluff and Hansen (1969) have ascribed the 1610, 1812, 1894, 1932 and 1950 earthquakes to the Boconó fault. Besides the 1610, 1812 and 1894 events, Aggarwal (1983) [later cited textually by McCann and Pennington (1990) and Suárez and Nábelek (1990)], also ascribed the 1644 and 1875 earthquakes to the Boconó fault. Seismotectonic associations of a few of these are still uncertain. For instance, Grases (1990) indicates a probable association of the Tocuyo 1950 earthquake with the Boconó fault, as Cluff and Hansen (1969) did. However, Choy (1998) and Audemard et al. (1999b) propose that other neighboring faults could also be potential sources because of the structural complexity in the epicentral region, located west of the Boconó fault (Fig. 1). Furthermore, Singer and Beltrán (1996) associate the 1644 Pamplona and 1875 Cúcuta earthquakes with the Pamplona indenter, and the 1644 event particularly with the Aguas Calientes fault; but with the BF. Conversely, the association of the 1610 and 1894 earthquakes with the southern segment of the Boconó fault has been recently confirmed by paleoseismic studies (Audemard, 1997a, b).

The present-day seismicity along the Boconó fault occurs within a broad zone, involving the entire width of the MA, suggesting that other faults may be seismogenic as well, such as the thrust structures building up the chain. For instance, the Guanare March 5, 1975 and the Ospino December 11, 1977 earthquakes of magnitudes mb 5.5 and 5.6, respectively, are the most recent and largest events associated with the Southern Andean Foothills thrust system (Piedemonte Oriental fault). The depth distribution of seismicity associated with the chain build-up demonstrates that the entire (first 20–25 km) brittle crust (bulk squeezing) is being deformed at present (Audemard and Audemard, 2002).

Earthquake focal mechanism solutions constrain present fault kinematics. Besides, the individual stress tensor derived from each solution matches well with the stress field derived by Audemard and Audemard (2002), where the east–west oriented σ_{Hmax} in the southern MA progressively changes to a NW–SE orientation to the north along the chain. Although the number of focal mechanism solutions is not large (Fig. 11), it distinctly shows the active strain partitioning. The focal mechanism solutions also confirm fault-slip determinations based on geologic criteria (discussed previously for both Boconó and foothills), since they locally exhibit mainly pure strike and reverse slip. For instance, focal mechanisms along the chain axis evidence essentially RLSS, whereas three mechanisms (solutions 25, 29 and 52 in Fig. 11) on the eastern side of the Andes (among them: the Guanare 1975 and the Ospino 1977 earthquakes) show dominant reverse slip.

All focal mechanism solutions displayed in Fig. 11 correspond to shallow moderate earthquakes. Most of them are below magnitude 5 and very few below 6. The focal mechanisms are distributed as follows (Audemard and Audemard, 2002): (a) 12 out of 36 solutions exhibit dextral slip on NE–SW trending nodal planes that could be associated with the Boconó fault or other sub-parallel faults; (b) 9 of them correspond to transtensional oblique slip; (c) 7 solutions display transpressional oblique slip; (d) 7 displays almost pure reverse dip-slip solutions, spread over the mountain belt; and (e) only 1 shows extensional dip-slip on normal faults paralleling and along the axis of the chain that could result from mountain spreading.

The 7 transpressional oblique-slip solutions are here discussed in detail because of the implications they have on constraining the strain partitioning mechanism occurring within the chain. Out of those 7 focal mechanisms, only two (solutions 16 and 29) are relevant to this study because they are within the MA. Among the others, 4 solutions correspond to shallow moderate earthquakes that are in the Curarigua-Arangues region and located northwest of the MA. The fifth solution has its epicenter located in the northeastern EC. The two solutions of interest correspond to earthquakes with epicenters lying on the two opposite MA flanks. On the northwestern MA front, a 4.9 magnitude earthquake occurred in May 13, 1968 at a depth of 29 km (Pennington, 1981; Audemard et al., 1999b). The one occurring on the other foothills happened in December 11, 1977 at a depth of only 2 km (Audemard et al.,

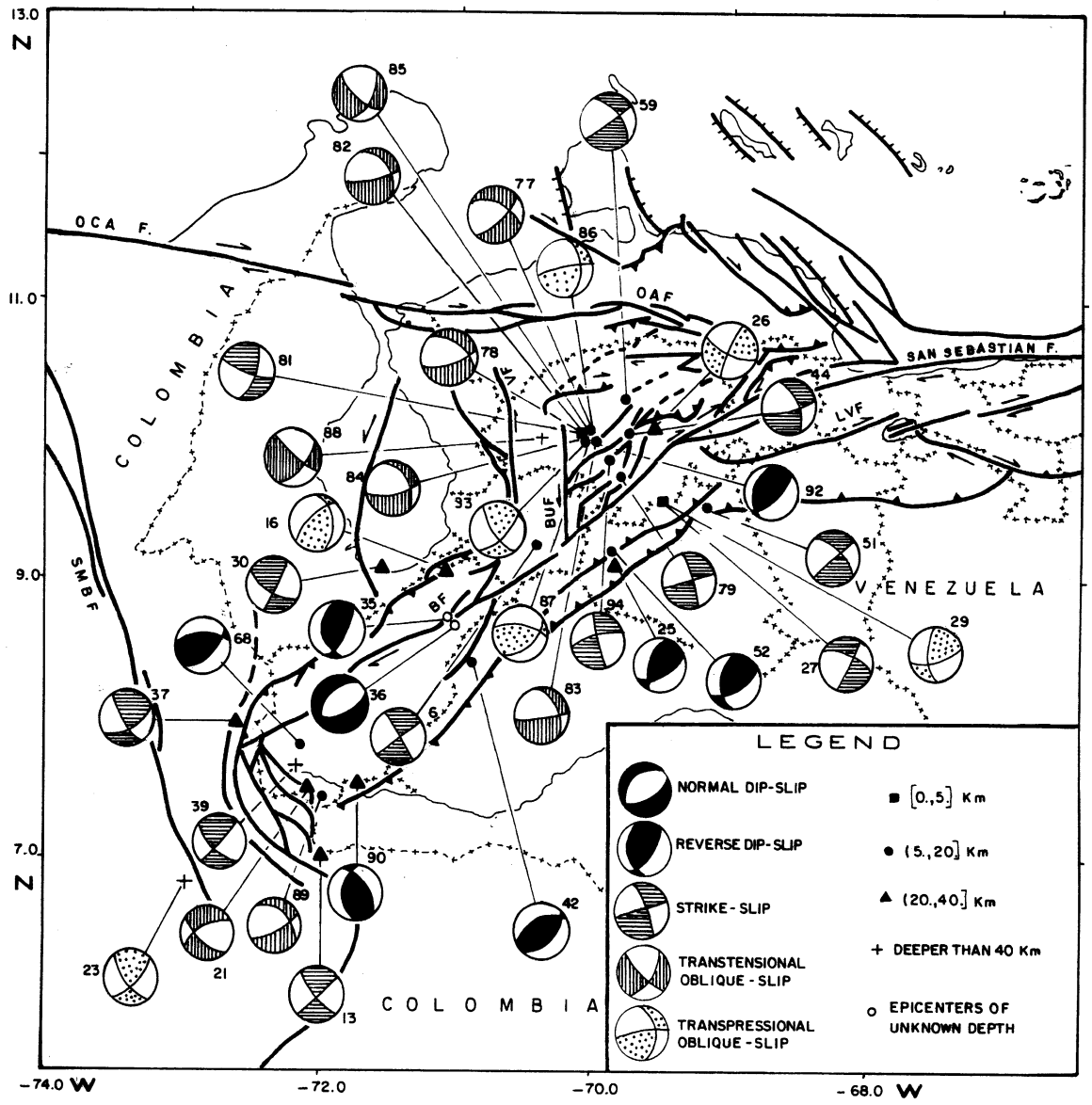

Fig. 11. Focal mechanism solutions for moderate shallow earthquakes located within or near the Mérida Andes, indicating the corresponding depth of the event (after Audemard et al., 1999b). Solutions are gathered based on their prevailing slip. Trajectories of σ_{Hmax} displayed in Fig. 12 are partly derived from these focal mechanism solutions, which also agree rather well with slip determined from neotectonic studies.

1999b). Consequently, very little transpressional oblique slip takes place within the MA chain and partitioning seems to be the actuating mechanism in the mountain belt.

9. Shortening vs. wrenching

9.1. Amount

The ratio of shortening to wrenching may give us clues about the significance of both deformation processes in the Andean orogeny. Audemard (1991) indicates that the southernmost Venezuela Andes has undergone a 14% shortening, of about 12 km, which should be considered as a lower bound. He also indicates that shortening across the Avispa massif (further northeastward; Figs. 1 and 9) would be of the order of 45 km (40%). Besides, the same author suggests that reconstructions across other portions of the Andes would lead to larger estimates. In fact, Colletta et al. (1997) derive shortening values that average 60 km. These derived values strongly depend on thrust dips, which are not well constrained at depth, thus being a crucial issue. Besides, it is hard to differentiate how much shortening actually occurred along those presently inverted normal faults from shortening accommodated by younger shortcut low-angle thrust faults; the latter being an additional mechanism proposed by Colletta et al. (1997). Moreover, a fundamental question needs to

be raised: are all those shortcut faults actual shortcut faults instead of high-angle reverse thrust faults later flattened (originally over 40–50° dip Jurassic normal faults)? Some discussion on the model proposed by Colletta et al. (1997) may offer some additional constraints on the reliability of their estimate based on reconstruction of balanced cross-sections. The following observations can be derived from their plate 1 (p. 785): (a) the dip of the graben-bounding faults in their restored section (Jurassic stage) is rather low and the graben is obviously asymmetric where NW-bounding faults consistently show higher dips. This clearly points out that they are proposing that Jurassic rifting generated by simple shear. They do definitely propose so since they define a major NW-dipping fault in both restored sections. This Jurassic structuration has fundamental implications in the future tectonic inversion of the graben, which needs to be kept in mind; (b) most crustal-scale reverse fault planes flattens when reaching upper crustal levels which should not be taken into account when calculating shortening because this is produced by topographic flattening of the chain due to gravity (chain "lateral spreading"), thus implying that actual shortening should be less than values proposed.

This conclusion can be reached by another way of reasoning. At present, the chain exposes Cretaceous rocks at about 2000 m in elevation within the hanging-wall block of the northwestern thrust front while the same sequence is buried under 8 km of younger deposits in the footwall compartment (Fig. 8A). Therefore, a minimum total uplift of the order of 10 km can be reasonably proposed for those Cretaceous rocks. However, let us assume that those rocks were removed by erosion from the higher areas of the chain. So, let us consider a total uplift of 13–15 km to be conservative. Assuming that the Jurassic faults had original dips of the order of 30°, which is rather low for a normal fault, the total shortening excluding any internal ductile deformation would be of some 40–50 km at most from simple trigonometric calculations. Therefore, estimates of 60 km might be overestimating the amount of shortening in some 20–25%, because mountain belt flattening has not been taken into account.

As much as 70–80 km of dextral wrench offsets in Mesozoic rocks have been measured along the Boconó fault. Stephan (1982) proposed cumulative dextral slip along this major fault of about 80 km, based on lateral offsets of the Caribbean nappes emplaced in the Eocene and outcropping in the northern termination of the MA. This value has been debated by Audemard (1993) based on the reliability of subhorizontal geologic markers for measuring horizontal displacements. More reliable and frequent dextral offsets are of the order of 30 km (see Giraldo (1989) for a more detail discussion; Audemard and Giraldo, 1997). An additional argument in favor of the total right-lateral slip along the Andes axis may be derived from the present locations of Bouguer anomaly minima in both flexural basins (Audemard and Audemard, 2002). These authors indicate that the southeastern foothills minimum is located between Capitanejo and Ciudad Bolivia (refer to gravimetric map by Bonini et al., 1977), exactly SE of the highest peaks of the Sierra Nevada; the latter in turn being south of the Boconó fault (in the southeastern half of the MA). Conversely, the northwestern foothills minimum is located near Caja Seca-Bobures (refer to Fig. 1 for relative location), being shifted northeastward 30 km with respect to both the other flank gravimetric minimum and the highest peaks of the MA. This RLSS estimate of Audemard and Audemard (2002) matches rather well with those proposed by Giraldo (1989) and Audemard and Giraldo (1997). Consequently, a wrenching/shortening ratio of 1:1 to 1:1.5 can not be neglected: 30 km of dextral wrenching against a shortening amount of the same order or under 50% higher (40–50 km).

9.2. Activation age

The age of onset of chain uplift has been determined by very different approaches and diverse techniques. Most agree that the present MA started to build-up sometime in the Late Miocene (Stephan, 1982; Audemard, 1991, 1993; Colletta et al., 1997, among others). The age of sedimentary growth wedges in both flanking flexural basins support this (Audemard, 1991; De Toni and Kellogg, 1993; Duerto et al., 1998). Uplift ages derived from apatite fission tracks by Kohn et al. (1984) and Shagam et al. (1984) support the sediment-derived ages, but also suggest uplift diachronism across the MA from southeast to northwest.

On the other hand, a reliable age of wrenching onset within the chain is not available yet because of lack of thorough sedimentary records for any of the pull-apart basins associated with the Boconó fault. Therefore, it has to be derived indirectly based on certain assumptions. For instance, Audemard (1993) proposed that RLSS within the MA is a direct consequence of the suturing related to the PA collision. This collisional process started at about 12 Ma, and a land bridge was achieved by 3 Ma. Another approach involves considering that the entire northwestern corner of SA (including most of the Ecuadorian, Colombian and part of the Venezuelan Andes) is split from cratonic SA by a long, complex dextral transform fault system, including the Pallatanga, Algeciras, Guaicaramo, Boconó and other minor faults (Case et al., 1971; Dewey, 1972; Pennington, 1981; Stephan, 1982; Audemard, 1993, 1998; Freymueller et al., 1993; Ego et al., 1996). The opening and deepening of the Jambelí graben in the Gulf of Guayaquil, offshore Ecuador, is related to the northward escape of northwestern SA (Audemard, 1993,

1998; Fig. 2). This basin, interpreted as a pull-apart, is mainly filled by Plio–Quaternary marine deposits, but sedimentation started in the Late Miocene (Benítez, 1986), thus constraining the initial age of wrenching (Audemard, 1993).

Therefore, thrusting, transcurrent slip and chain uplift (as bulk squeezing) in the MA seem to start at once, at the end of the Miocene, thus implying that the occurrence of partitioning is to be related to a single cause: the present stress tensor that results from major tectonic plate interactions (Fig. 12). Consequently, some 13–15 km of uplift and 30 km of wrenching have taken place in the last 3–5 Ma within the MA. So, the uplift rate ranges between 2.6 and 5.0 mm/a whereas wrenching rate varies between 6 and 10 mm/a.

An earlier estimate of uplift rate based on ages of cooling derived from apatite fission tracks by (Kohn et al., 1984; Fig. 12) indicated only 0.8 mm/a. This value seems very low compared to the estimate calculated above. Several factors could account for this discrepancy. First, all the vertical throw observed across the Cretaceous sedimentary rocks is not only due to tectonic uplift but some isostasy is taking place in response to chain erosion/denudation; but this could also apply to the El Carmen pluton, from where Kohn et al.'s (1984) uplift rate is derived. Second, the Cretaceous sedimentary rocks originally deposited on a differentiated topography, which could be the case because some arches have been described across the present trend of the MA, such as the Mérida arch. In that case, we would be overestimating the rate based solely on the measured vertical throw if no elevation correction is incorporated. However, the vertical throw should be at least in the order of 10 km. Third, the El Carmen pluton is affected by a set of imbricated thrusts but not raised as a single mass; thus, the slope of the elevation/age curve does not represent the average uplift rate of such pluton but only a lower bound. Shagam et al. (1984), based on geologic criteria, propose another curve for the Andes for the Plio–Pleistocene timespan, identified by "J" (their Fig. 13, p. 405) where almost 4000 m of uplift has taken place in about 0.8 Ma. Thus, an uplift rate of almost 5 mm/a can be calculated, a value that matches with our upper bound of uplift rate range. It is very likely that uplift rates may have increased through time, from the 0.8 mm/a value determined by Kohn et al. (1984) to the 5 mm/a proposed by Shagam et al. (1984) from geologic criteria, whereas our estimate is an average value (3.75 ± 1.25 mm/a) due to uncertainties (exact activation age of uplift and total uplift).

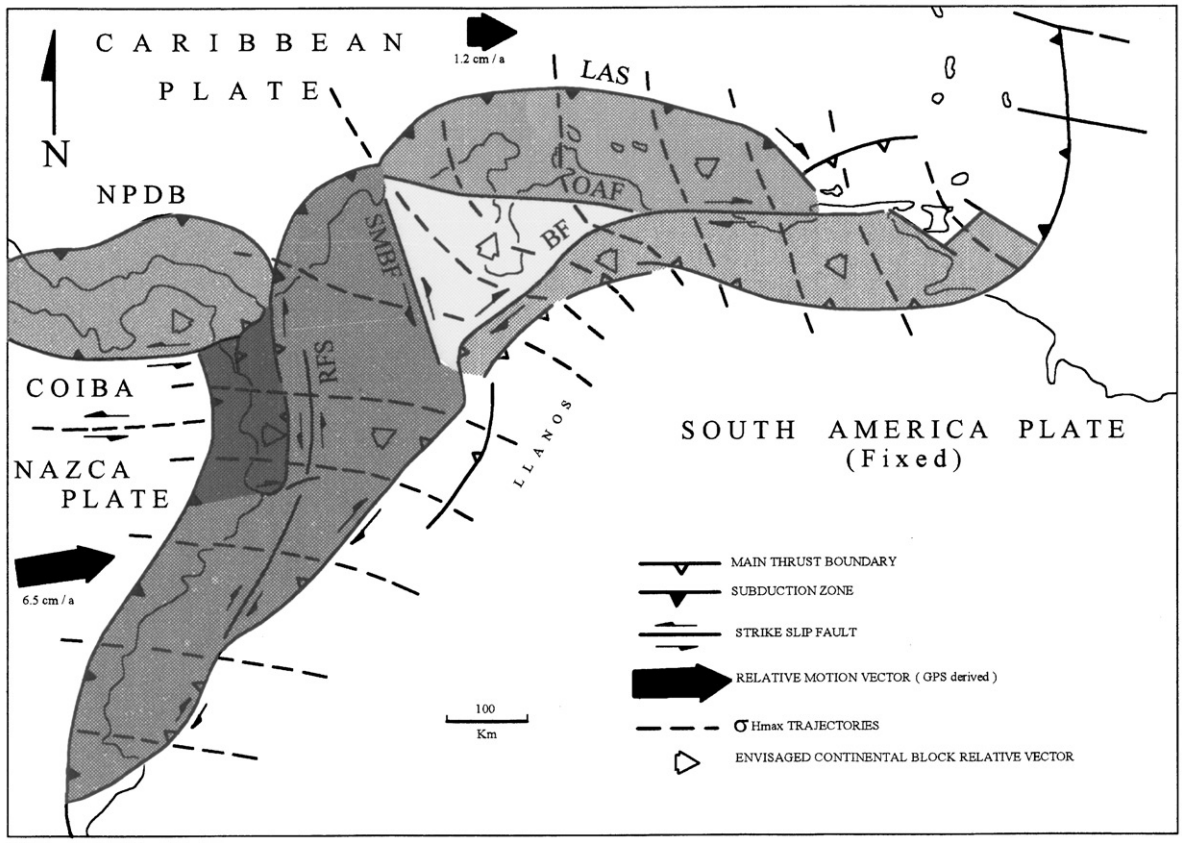

Fig. 12. Schematic geodynamic setting of northwestern South America, showing the maximum horizontal stress trajectories and relative motion vectors with respect to South America (active tectonics and trajectories modified from Taboada et al., 2000 and Beltrán, 1993, and Giraldo, 1989, respectively). Main continental tectonic blocks of northwestern SA are identified, and their interpreted kinematics with respect to SA are indicated.

10. Conclusions

Evidence of very distinct types has been discussed to show that the MA is an active feature in northwestern SA, where stress (strain) partitioning is driving the deformational evolution of this young chain since late Miocene–early Pliocene. Partitioning seems to be attested to by focal mechanism solutions of the present seismic activity, which is spread over the entire chain. Three major processes are taking place within the chain at present time, driven by complex plate interactions: transverse shortening, sub-parallel wrenching, and uplift. Even though considered as part of the Andes chain of South America, this chain is not of the Andean type because it is not directly related to type-B subduction. It is involved in an indentation–expulsion process that affects the entire northwestern corner of SA, and this chain seems to fit in the orogenic-float type. The indenter seems to be the Chocó block and San Jacinto terranes and the blocks in expulsion comprise the North Andes (most of Colombian Andes), the Panamá, the Maracaibo and the Bonaire blocks. In the orogenic-float model, the Andes sits between the MTB and the SA plate, being the boundary along the sub-axial RLSS Boconó fault. The stress field in northwestern SA varies as a function of what convergence vector among larger plates prevails (Nazca–SA or Caribbean–SA). The MA are subject to oblique compression, which simultaneously induces the three major processes mentioned above.

Numerous unequivocal evidence of active tectonics has been presented. Shortening across the chain is better imaged at the foothills due to the lack of young deformational markers in the chain core, even though chain-bounding thrust faults are frequently masked by triangular zones. However, a set of indirect ground deformations in the foothills collectively prove the occurrence of both thrusting and folding/flexing: (1) flexural scarps; (2) flights of alluvial terraces exclusively present in the hangingwall block; (3) drainage patterns and anomalies (such as radial drainages, densely dissected morphological scarps, river pattern inversion with flow from basin to range, river diversions, beheaded drainages and stream captures, changes in incision depth and river gradient along river course, dammed creeks and rivers, imbalances between current river flow and river gaps, wind gaps (abandoned river gaps) and tectonic "gutters"); and (4) progressive unconformities (increase of tilt of ground surface or stratigraphic dip with increasing age of Quaternary alluvial ramps and even older formations). Wrenching along the Boconó fault has been demonstrated by the identification and mapping of a large number of diagnostic geomorphic evidence of RLSS surface rupturing, known for years and largely published in the literature, and applied as well to other minor transcurrent faults within the chain. Active bulging or folding within the chain is almost impossible to prove unless evolution of landscape is considered. Lastly, ongoing uplift is attested by erosional or depositional staircased alluvial terraces, deep transverse-to-chain incision and disruption/cannibalization of pull-apart basins.

Wrenching along the Boconó fault seems to be in the order of some 30 km, whereas shortening across the chain should not exceed about 50 km. Slip rates of wrenching of 10 mm/a at most have been calculated, which match well with GPS estimates for the northeastward extrusion of the Maracaibo block with respect to South America. Earlier estimates of vertical slip rate in the Mérida Andes derived from elevation/age plots of apatite fission tracks are thought to be too slow (0.8 mm/a) and a more realistic value should be in the range of 2.5–5 mm/a

Acknowledgements

This contribution has been possible thanks to the invitation of Dr. Carlo Bartolini from the Università de Firenze to participate from the beginning as member of the Scientific Committee, and later as chairman of one of the sessions, of the Workshop "*Uplift and erosion: driving processes and resulting landforms*" that took place at Certosa di Pontignano (Siena, Italy) in September 20–21, 2001. His financial support is much appreciated, as well as Drs. Alessandro Michetti and Francesco Dramis' co-financing, from Universita dell'Insubria (Como) and Università di Roma 3 (Rome), respectively. My gratitude also is for my brother, and also geologist, Dr. Felipe Audemard for the fruitful discussion on Andean problems. This paper also took profit of my recent incursions in Colombia active tectonics, for which I am thankful to Drs. Hans Diederix (retired from ITC at Entschede, The Netherlands), Armando Espinosa from Universidad del Quindío (Armenia, Dpto. Del Quindío, Colombia) and Jairo Alonso Osorio from Ingeominas-Bogotá. China-ink hand-made drawings are solely the effort of Miss Marina Peña and some photo and figure scanning is a contribution of my young colleagues Engs. Raymi Castilla and Luis Melo; all three working for the Earth Sciences Department of Funvisis. Last but not least, my heartiest thanks to Funvisis that has financed all my field work up to present, in and around the Mérida Andes. Dr. Gianluca Valensise's comments substantially helped to improve the final draft of this contribution.

References

Aggarwal, Y., 1983. Seismic gaps and earthquake hazard in Venezuela. Proceedings of Simposio Neotectonica, Sisimicidad y Riesgo Geológico en Venezuela y el Caribe, Caracas, p. 26 (abstract).

Audemard, F.E., 1991. Tectonics of Western Venezuela. Ph.D. Thesis, Rice University, Texas, 245pp. plus appendices.

Audemard, F.A., 1993. Néotectonique, Sismotectonique et Aléa Sismique du Nord-ouest du Vénézuéla (Système de failles d'Oca-Ancón). Ph.D. Thesis, Université Montpellier II, France, 369pp. plus appendix.

Audemard, F.A., 1996. Contribución del Dr. Carlos Schubert Paetow (1983–94) al conocimiento de la Neotectónica del Caribe: visión crítica de un colega neotectonista. Boletín Sociedad Venezolana de Geólogos 21 (2), 23–37.

Audemard, F.A., 1997a. Holocene and historical earthquakes on the boconó fault system, southern Venezuelan Andes: trench confirmation. Journal of Geodynamics 24 (1–4), 155–167.

Audemard, F.E., 1997b. Los andes venezolanos, visión alterna. VIII Congreso Geológico, Venezolano, Vol. 1, Porlamar, pp. 85–92.

Audemard, F.A., 1998. Evolution Géodynamique de la Façade Nord Sud-américaine: Nouveaux apports de l'Histoire Géologique du Bassin de Falcón, Vénézuéla. XIV Caribbean Geological Conference, Vol. 2, Trinidad, pp. 327–340.

Audemard, F.A., 1999. Morpho-structural expression of active thrust fault systems in humid tropical foothills of Colombia and Venezuela. Zeitschrift für Geomorphologie 118, 1–18.

Audemard, F.A., 2000. Major active faults of Venezuela. 31st International Geological Congress, Rio de Janeiro, Brasil (extended abstract).

Audemard, F.E., Audemard, F.A., 2002. Structure of the Mérida Andes, Venezuela: relations with the South America–Caribbean geodynamic interaction. Tectonophysics 345 (1-4), 299–327.

Audemard, F.A., Giraldo, C., 1997. Desplazamientos dextrales a lo largo de la frontera meridional de la placa Caribe, Venezuela septentrional. VIII Congreso Geológico Venezolano, Vol. 1, Porlamar, pp. 101–108.

Audemard, F.A., Pantosti, D., Machette, M., Costa, C., Okumura, K., Cowan, H., Diederix, H., Ferrer, C., Sawop Participants, 1999a. Trench investigation along the Merida sectión of the Boconó fault (central Venezuelan Andes), Venezuela. In: Pavlides, S., Pantosti, D., Peizhen, Z. (Eds.), Earthquakes, Paleoseismology and Active Tectonics. Selected papers to 29th General Assembly of the Association of Seismology and Physics of the Earth's Interior (IASPEI), Thessaloniki, Greece, August 1997; Tectonophysics 308, 1–21.

Audemard, F.A., Romero, G., Rendón, H., 1999b. Sismicidad, Neotectónica y Campo de Esfuerzos del Norte de Venezuela. FUNVISIS' unpublished Report for PDVSA-CVP, Caracas, 221pp.

Audemard, F.A., Machette, M., Cox, J., Dart, R., Haller, K, 2000. Map and database of Quaternary faults in Venezuela and its offshore regions. US Geological Survey Open-File Report 00-0018, Includes map at scale 1:2,000,000 and 78pp.

Audemard, F.A., Beck, C., Carrillo, E., Cousin, M., Paterne, M., 2001. Sedimentary record of late Pleistocene seismic activity along the Boconó fault (Mérida Andes, Venezuela): the Los Zerpa moraine-dammed paleo-lake. Congrès 2001 de l'Association des Sédimentologues Français, Orléans (abstract).

Bell, J., 1972. Geotectonic evolution of the southern Caribbean area. Geological Society of America Memoir 132, 369–386.

Bellizzia, A., Pimentel, N., Bajo, R. (compilers), 1976. Mapa geológico-estructural de Venezuela, scale 1:500,000. Ministerio de Minas e Hidrocarburos. Foninves, Caracas.

Beltrán, C., 1993. Mapa Neotectónico de Venezuela. Scale 1:2,000,000. Funvisis, Caracas.

Beltrán, C., 1994. Trazas activas y síntesis neotectónica de Venezuela a escala 1:2.000.000. VII Congreso Venezolano de Geofísica, Caracas, pp. 541–547.

Benítez, S., 1986. Síntesis geológica del graben de Jambeli. IV Congreso Ecuatoriano de Geología, Minería y Petróleo, Vol. 1, pp. 137–160.

Boinet, T., 1985. La frontière méridionale de la plaque caraïbe aux confins colombo-vénézuéliens (Norte de Santander, Colombie): données géologiques. Ph.D. Thesis, Université de Paris VI, Paris, France, 204pp. plus appendices.

Boinet, T., Bourgois, J., Mendoza, H., Vargas, R., 1985. Lepoinçonde pamplona (colombie): un jalon de la frontière méridionale de la plaque caraïbe. Bulletin de la Societé Géologique de France 8 I (3), 403–413.

Bonini, W, Pimstein de Gaete, E., Graterol, V. (compilers), 1977. Mapa de anomalías de Bouguer de la parte norte de Venezuela y áreas vecinas. Scale 1:1,000,000. MEM, Caracas, Venezuela.

Cabello, O., 1966. Estudio geomorfológico del área de Mérida y sus alrededores. Unpublished undergraduate thesis, Faculty of Forestry Sciences, Universidad de Los Andes, Mérida, 140pp.

Casas, A., 1991. Estudio sismotectónico del valle del Yaracuy. Funvisis-Universidad de Zaragoza unpublished report, Caracas.

Casas, A., 1995. Geomorphological and sedimentary features along an active right-lateral reverse fault. Zeitschrift für Geomorphologie NF 39 (3), 363–380.

Casas, A., Diederix, A., 1992. El valle de Yaracuy (límites de la Placa Caribe, Venezuela): ejemplo de una cuenca cuaternaria asociado a una curvatura de falla. III Congreso Geológico de España y VIII Congreso Latinoamericano de Geología, Vol. 4, Salamanca, pp. 269–279.

Case, J.E., Durán, L., López, A., Moore, W., 1971. Tectonic investigations in western Colombia and eastern Panamá. Bulletin of the Geological Society of America 82, 2685–2712.

Castrillo, J., 1997. Structuration néogène du flanc nord-ouest des Andes vénézuéliennes entre Torondoy et Valera. Ph.D. thesis, Université de Pau et des Pays de l'Adour, 247pp. plus appendix.

Choy, J., 1998. Profundidad y mecanismo focal del terremoto de El Tocuyo, 1950. Revista Geográfica Venezolana 39 (1–2), 203–217.

Cluff, L., Hansen, W., 1969. Seismicity and Seismic Geology of Northwestern Venezuela, Vols. I and II. Woodward-Clyde & Associates' unpublished report for Shell de Venezuela, Caracas.

Colletta, B., Roure, F., De Toni, B., Loureiro, D., Passalacqua, H., Gou, Y., 1996. Tectonic inheritance and structural styles in the Merida Andes (western Venezuela). 3rd International Symposium on Andean Geodynamics, Saint-Malo, France, pp. 323–326.

Colletta, B., Roure, F., De Toni, B., Loureiro, D., Passalacqua, H., Gou, Y., 1997. Tectonic inheritance, crustal architecture, and contrasting structural styles in the Venezuelan Andes. Tectonics 16 (5), 777–794.

De Toni, B., Kellogg, J., 1993. Seismic evidence for blind thrusting of the northwestern flank of the Venezuelan Andes. Tectonics 12 (6), 1393–1409.

Dewey, J., 1972. Seismicity and tectonics of western Venezuela. Bulletin of the Seismological Society of America 62 (6), 1711–1751.

Duerto, L., Audemard, F.E., Lugo, J., Ostos, M., 1998. Síntesis de las principales zonas triangulares en los frentes de montaña del occidente venezolano. IX Congreso Venezolano de Geofísica (CD-Rom; paper # 25).

Ego, F., Sébrier, M., Lavenu, A., Yepes, H., Egues, A., 1996. Quaternary state of stress in the Northern Andes and the restraining bend model for the Ecuadorian Andes. Tectonophysics 259 (1-3), 101–116.

Ferrer, C., 1977. Estudio geomorfológico detallado de la cuenca media-inferior del Río Torbes, Edo. Táchira. Unpublished report, Faculty of Forestry Sciences, Universidad de Los Andes, Mérida, 180pp.

Ferrer, C., 1991. Características geomorfológicas y neotectónicas de un segmento de la falla de Boconó entre la ciudad de Mérida y la

Laguna de Mucubají, Estado Mérida. Guia de la excursión. Escuela Latinoamericana de Geofísica, 25.

Ferrer, C., Laffaille, J., 1998. El alud sísmico de La Playa: causas y efectos. El terremoto de Bailadores (1610). Revista Geográfica Venezolana 39 (1–2), 23–86.

Freymueller, J.T., Kellogg, J.N., Vega, V., 1993. Plate motions in the north andean region. Journal of Geophysical Research 98, 21853–21863.

Funvisis, 1997. Estudio neotectónico y geología de fallas activas en el piedemonte surandino de los Andes venezolanos (Proyecto INTEVEP 95-061). Funvisis' unpublished report for INTEVEP, SA, Caracas, 155pp. plus appendices.

Funvisis, 1999. (coord. Audemard, F. A.). Estudio de Neotectónica y Geología de Fallas Activas del Triángulo de Fallas de Boconó, Oca-Ancón y Valera (Proyecto INTEVEP 97-018). Funvisis' unpublished report for INTEVEP, SA, Caracas, 138pp. plus appendices.

Giegengack, R., 1984. Late cenozoic tectonic environments of the central Venezuelan Andes. Geological Society of America Memoir 162, 343–364.

Giraldo, C., 1985. Neotectónica y sismotectónica de la región de El Tocuyo-San Felipe (Venezuela centro-occidental). VI Congreso Geológico, Venezolano, Vol. 4, Caracas, pp. 2415–2451.

Giraldo, C., 1989. Valor del desplazamiento dextral acumulado a lo largo de la falla de Boconó, andes venezolanos. GEOS 29, 186–194.

Giraldo, C., Audemard, F.A., 1997. La cuenca de tracción de Cabudare, Venezuela centro-occidental. VIII Congreso Geológico Venezolano, Vol. 1, Porlamar, pp. 351–357.

González de Juana, C., 1952. Introducción al estudio de la geología de Venezuela. Boletín de Geología (Caracas) 2, 407–416.

Grases, J., 1990. Terremotos Destructores del Caribe 1502–1990. Orcyt (UNESCO), Montevideo, Uruguay, 132pp.

Gutscher, M-A., Spakman, W., Bijwaard, H., Engdahl, R., 2000. Geodynamics of flat subduction: seismicity and tomopraphic constraints from the andean margin. Tectonics 19 (5), 814–833.

Henneberg, H., 1983. Geodetic control of neotectonics in Venezuela. Tectonophysics 97, 1–15.

Hospers, J., Van Wijnen, J., 1959. The gravity field of the Venezuelan Andes and adjacent basins. Verslag van de Gewone Vergadering van de Afdeling Natuurkunde Koninklijke Nederlandse Akademie van Wetenschappen 23 (1), 1–95.

Jácome, M., 1994. Interpretación geológica, sísmica y gravimétrica de un perfil transandino. Undergraduate Thesis, Universidad Simón Bolívar, Caracas, Venezuela, 68pp.

Jordan, T., 1975. The present-day motions of the Caribbean plate. Journal of Geophysical Research 80, 4433–4439.

Kaniuth, K., Drewes, H., Stuber, K., Temel, H., Hernández, J.N., Hoyer, M., Wildermann, E., Kahle, H.G., Geiger, 1999. Position changes due to recent crustal deformations along the Caribbean–South American plate boundary derived from CASA GPS project. General Assembly of the International Union of Geodesy and Geophysics (IUGG), Birmingham, UK Poster at Symposium G1 of International Association of Geodesy.

Kellogg, J., Bonini, W., 1982. Subduction of the Caribbean plate and basement uplifts in the overriding South-American plate. Tectonics 1 (3), 251–276.

Kellogg, J., Vega, V., 1995. Tectonic development of panama, costa rica, and the colombian andes: constraints from global positioning system geodetic studies and gravity. Geological Society of America (Special Paper) Boulder, Colorado 295, 75–90.

Kohn, B., Shagam, R., Banks, P., Burkley, L., 1984. Mesozoic–Pleistocene fission track ages on rocks of the Venezuelan Andes and their tectonic implications. Geological Society of America Memoir 162, 365–384.

Lara, S., 1983. Estudio preliminar de las caracterísitcas sedimentológicas de los niveles de terrazas existentes en el área de La Grita, Estado Táchira. Síntesis Geográfica Universidad, Central de Venezuela 7 (14), 3–14.

Malfait, B., Dinkelman, M., 1972. Circum-caribbean tectonic and igneous activity and the evolution of the Caribbean plate. Geological Society of America Bulletin 83 (2), 251–272.

McCann, W., Pennington, W., 1990. Seismicity, large earthquakes, and the margin of the Caribbean plate. In: Dengo, D., Case, J.E. (Eds.), The Caribbean region. The Geology of North America, H. Geological Society of America, Boulder, Colorado, pp. 291–306.

Minster, J., Jordan, T., 1978. Present-day plate motions. Journal of Geophysical Research 83, 5331–5354.

Molnar, P., Sykes, L., 1969. Tectonics of the Caribbean and Middle America Regions from focal mechanisms and seismicity. Geological Society of America Bulletin 80, 1639–1684.

Padrón, C., Izarra, C., 1996. Modelo de velocidad 1D para el occidente de Venezuela. VIII Congreso Venezolano de Geofísica, Maracaibo, pp. 401–408.

Pennington, W., 1981. Subduction of the Eastern Panama basin and seismotectonics of Northwestern South America. Journal of Geophysical Research 86 (B11), 10753–10770.

Petróleos de Venezuela—PDVSA, 1992. Imagen Atlas de Venezuela, 1st Edition. Editorial Arte, Caracas, Venezuela. 271pp.

Pindell, J., Dewey, J., 1982. Permo-Triassic reconstruction of western Pangea and the evolution of the Gulf of Mexico/Caribbean region. Tectonics 1 (2), 179–211.

Rod, E., 1956a. Strike-slip faults of northern Venezuela. American Association of Petroleum Geologists Bulletin 40, 457–476.

Rod, E., 1956b. Earthquakes of Venezuela related to strike slip faults? American Association of Petroleum Geologists Bulletin 40, 2509–2512.

Rod, E., 1960. Comments on "the gravity field of the Venezuelan Andes and adjacent basins". Boletín Informativo Asociación Venezolana de Geología, Minería y Petróleo 3, 170–175.

Salgado-Labouriau, M., Schubert, C., Valastro, S., 1977. Paleoecologic analysis of a late Quaternary from Mucubají, Venezuelan Andes. Journal of Biogeography 4, 313–325.

Sánchez, M., Audemard, F.E., Giraldo, C., Ruiz, F., 1994. Interpretación sísmica y gravimétrica de un perfil a través de los Andes venezolanos. Memorias VII Congreso Venezolano de Geofísica, 251–258.

Schubert, C., 1968. Geología de la región de Barinitas-Santo Domingo. Andes Venezolanos Surorientales. Boletín de Geología, Caracas, 10, 161–181.

Schubert, C., 1976. LAS Mesas de Timotes y su edad. Revista Líneas 230, 8–12.

Schubert, C., 1980a. Morfología neotectónica de una falla rumbo-deslizante e informe preliminar sobre la falla de Boconó, Andes merideños. Acta Científica Venezolana 31, 98–111.

Schubert, C., 1980b. Late Cenozoic pull-apart basins, Boconó fault zone, Venezuelan Andes. Journal of Structural Geology 2 (4), 463–468.

Schubert, C., 1982. Neotectonics of the Boconó fault, western Venezuela. Tectonophysics 85, 205–220.

Schubert, C., 1983. La cuenca de Yaracuy: una estrucutra neotectónica en la región centro-occidental de Venezuela. Geología Norandina 8, 194–202.

Schubert, C., 1984. Basin formation along Boconó-Morón-El Pilar fault system, Venezuela. Journal of Geophysical Research 89, 5711–5718.

Schubert, C., Valastro, S., 1980. Quaternary Esnujaque Formation, Venezuelan Andes: preliminary alluvial chronology in a tropical mountain range. Zeitschrift der Deutschen Geologischen Gesellschaft 131, 927–947.

Schubert, C., Vivas, L., 1983. El Cuaternario de la cordillera de Mérida, Andes Venezolanos, 1st Edition. ULA-Fundación Polar, Mérida, Venezula, 345pp.

Shagam, R., Kohn, B., Banks, P., Dasch, L., Vargas, R., Rodríguez, G., Pimentel, N., 1984. Tectonic implications of Cretaceous–Pliocene fission track ages from rocks of the circum-Maracaibo Basin region of western Venezuela and eastern Colombia. Geological Society of America Memoir 162, 385–412.

Singer, A., 1998. Evaluación retrospectiva de los efectos geológicos destructoires del terremoto de 1610 en los Andes Venezolanos del siglo 17 y de observaciones de campo actuales. Revista Geográfica Venezolana 39 (1-2), 289–296.

Singer, A., Audemard, F.A., 1997. Aportes de Funvisis al desarrollo de la geología de fallas activas y de la paleosismología para los estudios de amenaza y riesgo sísmico. In: Grases, J. (Ed.), Diseño sismorresistente. Especificaciones y criterios empleados en Venezuela. Publicación Especial Academia de las Ciencias Naturales, Vol. 33. Matemáticas y Físicas, Caracas, pp. 25–38.

Singer, A., Beltrán, C., 1996. Active faulting in the Southern Venezuelan Andes and Colombian borderland. Proceedings of the Third International Symposium on Andean Geodynamics, Saint-Malo, France, pp. 243–246.

Singer, A., Lugo, M., 1982. El alud sísmico del 3-02-1610 en el valle del Mocotíes (Andes Venezolanos). Confrontación de los testimonios del siglo XVII y de las evidencias de campo actuales. Acta Científica Venezolana 33, 214 (abstract).

Soulas, J.-P., 1985. Neotectónica del flanco occidental de los Andes de Venezuela entre 70°30′ y 71°00′W (Fallas de Boconó, Valera, Piñango y del Piedemonte). VI Congreso Geológico Venezolano, Vol. 4, Caracas, pp. 2690-2711.

Soulas, J.-P., 1986. Neotectónica y tectónica activa en Venezuela y regiones vecinas. VI Congreso Geológico Venezolano, Caracas-1985 10, 6639–6656.

Soulas, J.-P., Singer, A., 1987. Mapa ''Evidencias de actividad cuaternaria en las fallas''. In: Soulas, J.-P., Singer, A., Lugo, M. (Eds.), Tectónica cuaternaria, características sismogénicas de las fallas de Boconó, San Simón y del piedemonte occidental andino y efectos geológicos asociados a la sismicidad histórica (Proyecto Sumandes). Funvisis' unpublished report for Maraven SA, 90pp., Caracas.

Soulas, J.-P., Rojas, C., Schubert, C., 1986. Neotectónica de las fallas de Boconó, Valera, Tuñame y Mene Grande. Excursión No. 4. VI Congreso Geológico Venezolano, Vol. 10, Caracas, pp. 6961–6999.

Stephan, J.-F., 1982. Evolution géodinamique du domaine Caraïbe, Andes et cha⩽ne Caraibe sur la transversale de Barquisimeto (Vénézuéla). Ph.D. Thesis, Paris, 512pp.

Suárez, G., Nábelek, J., 1990. The 1967 Caracas earthquake: fault geometry, Direction of rupture propagation and seismotectonic implications. Journal of Geophysiscal Research 95 (B11), 17459–17474.

Sykes, L., McCann, W., Kafka, A., 1982. Motion of Caribbean plate during last 7 million years and implications for earlier Cenozoic movements. Journal of Geophysical Research 87 (B13), 10656–10676.

Taboada, A., Rivera, L.A., Fuenzalida, A., Cisternas, A., Philip, H., Bijwaard, H., Olaya, J., Rivera, C., 2000. Geodynamic of the northern Andes: Subductions and intracontinental deformation (Colombia). Tectonics 19 (5), 787–813.

Tapponnier, P., 1977. Evolution tectonique du système alpin en méditerranée: poinçonnement et écrasement rigide-plastique. Bulletin Societé Géologique de France 7 XIX (3), 437–460.

Tricart, J., Millies-Lacroix, A., 1962. Les terrasses quaternaires des Andes vénézuéliennes. Bulletin Société Géologique de France 7 (4), 201–218.

Tricart, J., Michel, M., 1965. Monographie et carte géomorphologique de la région de Lagunillas (Andes vénézuéliennes). Revue de Géomorphologie, Dynamique 15, 1–33.

Wadge, G., Burke, K., 1983. Neogene Caribbean plate rotation and associated central American tectonic evolution. Tectonics 2 (6), 633–643.